Palaeogeography, Palaeoclimatology, Palaeoecology
November 2022, Volume 605, Pages 111232 (13p.)
https://doi.org/10.1016/j.palaeo.2022.111232
https://archimer.ifremer.fr/doc/00794/90602/

Response of vegetation to hydroclimate changes in northeast Brazil over the last 130 kyrs

Piacsek Patricia [1, *], Behling Hermann [3], Stríkis Nicolás M. [5], Ballalai João M. [4, 5], Venancio Igor M. [5], Da S. Rodrigues Alice Maria [5], Albuquerque Ana Luiza S. [2]

[1] Centro de Geociencias, Universidad Nacional Autónoma de México (UNAM), Blvd. Juriquilla 3001, Campus UNAM 3001, 76230 Juriquilla, Querétaro, Mexico
[2] Programa de Pós-Graduação Dinâmica dos Oceanos e da Terra (DOT-UFF), Fluminense Federal University, Av. Gen. Milton Tavares de Souza s/n°, Gragoatá, Campus da Praia Vermelha, 24210346 Niterói, RJ, Brazil
[3] Department of Palynology and Climate Dynamics, University of Göttingen (UG), Untere Karspüle 2, 37073 Göttingen, Germany
[4] UMR 6538 Geo-Ocean, CNRS, IFREMER, UBO, UBS, Centre de Bretagne, 29280 Plouzané, France
[5] Geoquímica Ambiental, Fluminense Federal University (UFF), Outeiro São João Batista, s/n – 5° andar Instituto de Química, Campus do Valonguinho Centro, 24020141 Niterói, RJ, Brazil

* Corresponding author : Patricia Piacsek, email address : Piacsekpatricia@geociencias.unam.mx

Abstract :

In this paper, we use palynology and geochemical proxies to reconstruct late Quaternary vegetation changes within the hydrographic basin of Parnaíba, Northeast Brazil, over the last 130 kyrs. Findings are based on the analysis of a marine sediment core (GL-1248) retrieved from the western equatorial Atlantic (0°55.2′S, 43°24.1′W), close to the coast. Geochemical proxies (Fe/K ratio and ƐNd) indicative of soil erosion match changes in reconstructed vegetation, suggesting a dynamic pattern of hydrological disturbances and ecosystem evolution. Given that reconstructed vegetation does not present the same response to precipitation anomalies on the millennial scale, we sought the main drivers of vegetation changes in the Parnaíba watershed. Results indicate that vegetation succession was primarily influenced by austral insolation from March to May, which triggered changes in the pioneer vegetation types. Our study improves the knowledge of tropical vegetation dynamics in an orbital framework, suggesting 23-kyr precessional cycles as the main driver of landscape evolution in Northeast (NE) Brazil. We also infer that such past climate change events may have been a key causal factor of the high biodiversity of the Neotropics, mediated through the biological exchange of the Amazon and Atlantic rainforest species via ecological forest corridors in the semi-arid Northeast Brazil.

Highlights

► We discuss vegetation change and how it reflects hydrological changes within the Parnaíba Basin, northeastern (NE) Brazil, over the past 130 kyrs ► Geochemical proxies (Fe/K ratio and ƐNd) in core GL-1248 are synchronous with reconstructed vegetation patterns, highlighting periods of enhanced or reduced local soil erosion during hydrological disturbances ► We define three major vegetation groups (tropical dry forest, lowland rainforest, and wetland), and the discrepancy in water requirements between tropical dry forests and lowland rainforests is discussed ► Analysis of the hydroclimatic mechanisms in NE Brazil that triggered the succession of vegetation during glacial phases is discussed

Keywords : Marine-based palynology, Northeastern Brazil, Soil Erosion, Vegetation reconstruction, Glacial-interglacials, Climate change

1 Introduction

Many hypotheses have discussed the mechanisms that led to the current rainforest distribution and its plant diversity (Colinvaux et al., 1996; Cárdenas et al., 2011; Antonelli et al., 2011; Cohen et al., 2014). Hoorn et al. (2010) showed that the merger between climate, bedrock, and edaphic conditions over the different Amazon basin units is highly relevant to explain the actual biodiversity. Por et al. (1992) proposed at least three different pathways that may have connected the Amazon forest with the Atlantic coastal rainforest (Northwest–Southeast of South America, coastal route of Northeastern Brazil, and montane route of Northeastern Brazil). Phylogenetic and palynological studies point to ancient connections between the two forests and indicate that both coastal and montane NE routes had gained relevance during the Quaternary climate episodes (Fig. 1) (Batalha et al., 2013). The influence of climate change on vegetation diversification has been considered regarding the richness of Neotropical biodiversity (Por et al., 1992; Ledo & Colli, 2017; Silveira et al., 2019). Hydrological changes over the Plio-Pleistocene may have promoted the spatial change in the distribution of the gallery forests and the series of deciduous and semi-deciduous forest patches bridging the Amazon and Atlantic rainforests (de Oliveira et al., 1999; Behling et al., 2000; Costa, 2003; Pinaya et al., 2019; Piacsek et al., 2021b).During the last glacial period, those hydrological changes over the NE of South America were mainly governed by millennial-scale displacements of the Intertropical Convergence Zone (ITCZ) position and widely related to events known as Heinrich Stadials (HS) (Wang et al., 2004; Stríkis et al., 2018). The HS was depicted as an abrupt and extensive freshwater intrusion into the North Atlantic (Heinrich, 1988; Hemming, 2004), weakening the Atlantic Meridional Overturning Circulation (AMOC), with accentuated meridional sea surface temperature (SST) gradients and reduced inter-hemispheric

energy transport (Burkel et al., 2015; Mulitza et al., 2017). Consequently, the atmospheric conditions rearranged with significant meridional changes in the intensity of trade winds and the ITCZ mean position (Deplazes et al., 2013). When the NE trade winds gained strength, warm superficial waters were restricted at the western equatorial Atlantic and probably enabled the permanence of the ITCZ at a more southward position, bringing Atlantic moisture onto the continent (Broccoli et al., 2006; McGee et al., 2018; Utida et al., 2019).

Within some HS events, underlining HS 1, the palynological records of the marine sediment core GeoB 3104-1 pointed to an increase in the relative abundance of rainforest pollen grains (e.g., *Alchornea*, Moraceae, Arecaceae, and others), suggesting an expansion of forests in NE Brazil (Behling et al., 2000). Jennerjahn et al. (2004) investigated high-resolution geochemical proxies (Fe/Ca and Ti/Ca) in the same marine core and identified millennial-scale sedimentation pulses related to the Younger Dryas (YD) and HS 1 to HS 8. The study identified the rise of pollen influx with a 1 to 2 kyr delay post-HS events, followed by the Fe/Ca ratio decrease, and suggested that the erosion was impaired post the development of the rainforest vegetation. Although both studies reconstructed the vegetation of NE Brazil using pollen resolution (52 samples at intervals of 10 cm) in which 24 sediment samples covered the temporal range of 42 kyr to 20 kyr, other studies of past vegetation dynamics in NE Brazil have highlighted the plasticity of the rainforest vegetation with a high pollen resolution within HS 1 (40 samples at intervals of 2–3 cm) and the YD (47 samples at intervals of 5 cm) (Dupont et al., 2010; Bouimetarhan et al., 2018). Both vegetation reconstructions were placed in different marine sediment cores over NE Brazil and pointed out the enhancement of rainforest in two steps within high precipitation levels on a millennial scale. Both studies are restricted to the vegetation change within one millennial-scale precipitation

anomaly. Here, we provided the reconstructed vegetation with a higher resolution than the GeoB 3104-1 record for the last glacial period. The new pollen record of the marine sediment core GL-1248 will provide the vegetation changes in the Hydrographic Basin of Parnaíba (HBP) for the last ~130 kyr. We focus on three major vegetation groups (tropical dry forest, lowland rainforest, and wetland) and how the ecosystem shifts are related to the soil erosion processes within the HBP. The discrepancy in water requirements between tropical dry forests and lowland rainforests is discussed, reflecting the hydroclimatic mechanisms in NE Brazil that triggered the vegetation change over the last glacial period.

2 The study area

The marine sediment core GL-1248 (0°55.2'S, 43°24.1'W) was retrieved from the continental slope (2264 m below sea level) off NE Brazil, located at a distance of about 160 km from the modern coastline and about 280 km from the fan of the Parnaíba River (Fig. 2). The Parnaíba River plume flows northward at the sea surface, transported by the North Brazil Current (NBC). The NBC is the superficial layer of the western boundary current and the main component for transporting heat to high latitudes of the North Atlantic. Its formation occurs at 10°S from the South Equatorial Current (SEC) bifurcation. The northern excursions of the ITCZ and stronger southeast trade winds strengthen the NBC transport during the austral winter (Stramma et al., 1995; Johns et al., 1998).

The arrival of the austral autumn (March–April–May) marks the southernmost position of the ITCZ (2°S) (Shimizu et al., 2021) in response to the seasonal warming of the adjacent tropical Atlantic Ocean. The ITCZ reaches the HBP during this time and triggers the highest Parnaíba River discharge. The HBP is located between the coordinates 02°21'S and 11°06'S latitude and 47°21'W and 39°44'W longitude and

shelters three states (Ceará, Maranhão, and Piauí). The HBP has an area of 340,000 km^2, and it is recognized as an ecotone zone with extensive areas of vegetation transitions, where the landscape evolution is highly dependent on the precipitation amount (Castro et al., 1998). Correia Filho et al. (2019) showed a median and interquartile range of seasonal rainfall variability of biomes in NE Brazil from 1979 to 2013: Amazon rainforest (1847.9 mm ± 418.7 mm), *caatinga* (773.1 mm ± 212.5 mm), *cerrado* (1196.6 mm ± 218.9 mm), and Atlantic rainforest (1363.8 mm ± 217.0 mm).

The *caatinga* has distinct vegetation physiognomic types such as xeric shrubland, shrub woodland, deciduous trees, and other drought-tolerant plants (Kuhlmann, 1977; Cole, 1986). It is highly represented by trees that belong to the Anacardiaceae (e.g., *Astronium, Schinopsis*), Apocynaceae (*Aspidosperma*), Malvaceae, and Fabaceae (e.g., *Ambulana, Caesalpinia, Calliandra, Senna, Mimosa, Pithecellobium*) (Bouimetarhan et al., 2018). Both biomes (*caatinga* and *cerrado*) may overlap in the transition zones. The *cerrado* (savanna to tropical dry forest) separates the *caatinga* (typical semi-arid dry forest) from the Amazon rainforest and is characterized by the occurrence of *Byrsonima*, *Mimosa*, and *Didymopanax* (Bouimetarhan et al., 2018). The lower part of the HBP has a perennial regime of superficial water flow with humid forest and extensive floodplains covered by herbaceous vegetation, swamps, and gallery forests (Lima & Melo 1985), marked by the presence of Moraceae-Urticaceae, Cyperaceae, and *Mauritia* (Ledru et al., 2002).

3 Material and methods

3.1 X-ray fluorescence Ti/Ca and Fe/K ratio

Sediment chemistry was analyzed by scanning the core surface of the archive half with X-ray Fluorescence (XRF) Core Scanner II (AVAATECH Serial No. 2) at the MARUM, University of Bremen (Germany) (Venancio et al., 2018). The XRF data

were measured downcore every 0.5 cm of GL-1248 for the chemical elements Al, Si, K, Ca, Ti, Mn, Fe by measuring their characteristic radiation. The elements were selected according to the distribution of major elements in Atlantic surface sediments (Govin et al., 2012). The Ca fluxes in this environment are derived mainly from biogenic $CaCO_3$ shells, and changes in Ca concentrations are most likely due to dilution by non-carbonate sediments (Govin et al., 2012; Nace et al., 2014). In contrast, Ti and Fe are mostly found in the soil residing in heavy minerals. During rainy periods and substantial runoff, the soil is revolved, carrying Ti and Fe, lined up with some siliciclastic material of fluvial origin (Govin et al., 2012). Among the available elements, the Ti/Ca ratio was used to indicate the erosion and soil contribution to the marine sediment core (Arz et al., 1998; Jennerjahn et al., 2015), and peaks of the Fe/K ratio were used to indicate relation to deep weathering process during wet periods (Mulitza et al., 2008).

3.2 Chronology

The age model of the GL-1248 was defined based on 12 analyses of radiocarbon dating using Accelerator Mass Spectrometry (AMS) measurements for the upper 550 cm (Venancio et al., 2018). For radiocarbon dating, we used two planktonic foraminifera types, *Globigerinoides ruber* and *Trilobatus sacculifer* (>150 mm), and it was performed at the Beta Analytic Radiocarbon Dating Laboratory, USA. The radiocarbon ages were calibrated with the IntCal13 calibration curve (Reimer et al., 2013), with a reservoir age of 400 ± 200 years (2σ) with no additional local reservoir effect (ΔR = 0) (Mulitza et al., 2017). The downcore ages were modeled using the software clam 2.2 (Blaauw, 2010), where 1665 to 564 cm correspond to 128 to 40 kyr, respectively. Most of the tie points were located at the midpoint between the alignment of the major Ti/Ca fluctuations and the abrupt oscillations of the $\delta^{18}O$ isotopes from the ice cores of the North Greenland Ice Core Project (NGRIP members, 2004). The core

GL-1248 is ~19 m long and spans the interval between 2 and ~130 kyr. The complete age-depth model was published in Venancio et al. (2018) (Fig. S1 and S2).

3.3 Palynological sample preparation

The sediment samples were prepared for pollen and spores analysis using 4-6 g (wet weight) following the standard laboratory procedures (Faegri & Iversen, 1989), excluding acetolysis. The sediment samples were sieved with a 150 µm mesh to remove the larger particles, such as shells and small stones. After that, one tablet of exotic *Lycopodium clavatum* spores (20848 ± 1546) was added to each sample to estimate the concentration (grains/cm³) and pollen influx (grains/cm²/yr) values (Stockmarr et al., 1971). The samples were treated with hydrochloric acid (HCl, 35%) for decalcification and cold hydrofluoric acid (HF, 40%) to remove the siliceous content. After the chemical treatment, samples were moved to an ultrasonic bath (maximum 30 seconds) for organic matter disaggregation. The samples were sieved with a 1 µm nylon mesh to remove small particles. The samples were processed at the Department of Palynology and Climate Dynamics, University of Göttingen (Germany).

3.4 Palynological analysis

A total of 140 sediment samples were collected from the GL-1248 core, following the Ti/Ca ratio peaks as an indicator of the primary source of the continental deposition as previously reported in Piacsek et al., (2021a). The pollen and spores were identified according to the reference collections of the Department of Palynology and Climate Dynamics (Göttingen, Germany). Pollen grains and spores were counted separately, each to a minimum of at least 100. An average of ~175 pollen grains and ~180 spores was counted per sample, with relative low concentrations during both interglacials. The pollen and spore concentration refers to the number of grains per unit volume of sediment, calculated for each sample by following the equation of

Benninghoff (1962). The concentration can be converted to the influx of pollen and spore, a measure of the number of pollen grains incorporated into the sediment per year (grains/cm^2/yr). For continental records, the fossil pollen and spore influx provide a potential proxy for quantitative biomass and population reconstructions (Davis and Deevey, 1964). However, factors other than biomass may affect the pollen influx of marine pollen records and must be interpreted carefully.

3.5 Vegetation groups

The palynological quality in the marine core GL-1248 reflects the different biomes of the Parnaíba watershed, with little influence of sea-level changes on the continental shelf. Palynological studies from NE Brazil for the last glacial period to the Holocene used ecological groups (de Oliveira et al., 1999; Behling, 2004; Ledru et al., 2006; Bouimetarhan et al., 2018). The most representative pollen groups were wetland, tropical dry forest (with the main recurrent taxa from *caatinga* and/or *cerrado* biomes), and lowland rainforest. The pollen types included for the wetland, lowland rainforest, and tropical dry forest groups are listed in Table 1, and the complete chart of pollen and spores can be found in the supplementary material (Fig. S3 to S9).

4 Results

4.1 Pollen sum, pollen concentration, sedimentation rate, and pollen influx

The total pollen sum accounts for arboreal pollen (AP) and nonarboreal pollen (NAP). The maximum sum of pollen counted per sample reached about 340, and the lowest value of pollen sum was ~100, with a mean value of ~175, illustrated by the red cut line (Fig. 3A). The pollen concentration in GL-1248 varied downcore from ~80 to 2200 grains/cm³ (average ~565 grains/cm³). During the glacial period, the lowest values of pollen concentrations were found from 55 to 40 kyr, indicating relatively reduced riverine contribution to the sediment core (Fig. 3B). In contrast, the sedimentation rate of the marine core GL-1248 displayed higher values during Marine Isotope Stage (MIS) 3 (~65 cm/kyr). Lower values were found during the interglacials and early glacial (~3 cm/kyr), with a mean sedimentation rate of 22 cm/kyr (Fig. 3C) (Venancio et al., 2018). We used the sedimentation rate to calculate the pollen influx, which varied from ~5.5 to ~1470 grains/cm^2/yr (average 160 grains/cm^2/yr) (Fig. 3D). However, the pollen signal of pollen influx was disguised by the sedimentation rate as the marine core was located at the continental slope and suffered a significant influence from the past sea-level oscillations (Fig. 3E) (Waelbroek et al., 2002). The palynological content was not sufficient (< 100 pollen grains per sample) for appropriate analysis for the section between ~100 to 90 kyr (1486 cm to 1392 cm) and between 7 to 2 kyr (80 cm to 23 cm). Due to the hiatus in core GL-1248 (~27 to ~16 kyr), the reconstruction of vegetation was not performed for the Last Glacial Maximum.

4.2 Relative abundances of pollen and spore grains

A total of 96 pollen taxa and 38 spores were identified. The relative abundance of pollen was calculated based upon the total pollen sum, and we used the total spores sum to calculate the relative abundance of spores. Following 12 pollen types present in

the most representative groups (wetland, lowland rainforest, and tropical dry forest) are highlighted due to their higher relative abundance: Cyperaceae (~38%), Malpighiaceae (~17%), Arecaceae (~13%), Asteraceae (~11%), Arecaceae *Mauritia* (~4,6%), *Borreria* (~8%), Mimosaceae (~5%), Moraceae–Urticaceae (~7,5%), Anacardiaceae (5%), *Alchornea* (~5%) Amaranthaceae *Gomphenera-Pfaffia* (~4,5%) Amaranthaceae/Chenopodiaceae (~4%) (Fig. 4). The higher relative abundance of spores are as follows: Cyatheaceae spp. sum (~39%), *Selaginella* (~20%), *Cyathea hemitelia* (~14%), Tree fern (~8%), and Trilete reworked (~31,5%) (Fig. S3). The higher relative abundance of Cyperaceae pollen occurred during the MIS 4 (~70 to ~60 kyr, or 1132 cm to 1022 cm) (Fig. 4). The completed pollen and spore diagrams are found on the supplementary material (Fig. S3 to S5), and the pollen data of GL-1248 were previously addressed in Piacsek et al. (2021).

The percentage of the main pollen groups (tropical dry forest, lowland rainforest, and wetland) are displayed with a black line referring to their respective pollen concentration. The pollen concentration in the marine core GL-1248 was low, mainly due to the amount of sediment processed to reach a minimum of 100 pollen units per sample. Furthermore, the pollen concentration depends on pollen production and transport efficiency (Maher, 1981). The pollen concentration of the wetland group was increased within the MIS 4, achieving higher values (~180 grains/cm³) than its total average (~90 grains/cm³). As previously mentioned, the lowest pollen concentration was found from 55 to 40 kyr, however, the pollen concentration of tropical dry forest (average of 75 grains/cm³) was superior to that of the lowland rainforest (average of 50 grains/cm³).

5 Discussion

5.1 The landscape changes and their implications for soil erosion within the HBP

We have established the age model of the GL-1248 core based on radiocarbon dates up to ~40 kyr and by the alignment between the peaks of Ti/Ca ratio and $\delta^{18}O$ isotopes well marked in the NGRIP over the last 130 kyr (Venancio et al., 2018) (Fig. 5A). During HS events, the western Atlantic ITCZ migrated to the southernmost position and contributed to enhancing local river catchments. In this sense, high Ti/Ca ratio values from GL-1248 suggest prolonged precipitation events over NE Brazil and a substantial contribution from rivers to the adjacent ocean (Fig. 5B) (Govin et al., 2012; Nace et al., 2014).

Periods of intense precipitation in NE Brazil enhanced the deep weathering and are also related to high Fe concentrations in the marine sediment compared to the more soluble K (Govin et al., 2012; Nace et al., 2014). Thus, we concluded that rapid increases in the Fe/K ratio of GL-1248 (Fig. 5C) are also related to precipitation anomalies over NE Brazil and intense weathering within the HBP. At the same time, the Fe/K is detached from the age model avoiding circularity in the reasoning. We found lower values of Fe/K during warmer interglacials, but the YD and substage MIS 5d (~110 kyr) depicted an increase of Fe/K. However, Fe/K was not depicted as during glacial Stadials, which might be explained by the increased distance between the coastline and the GL-1248 sediment core due to the rise in sea level during the interglacials (Fadina et al., 2019; Piacsek et al., 2021a). The higher sea levels flooded the continental shelf and hampered the arrival of terrigenous material to the location of the marine core as corroborated by the low pollen content for the interglacials.

The precipitation anomalies of the last glacial period enhanced the Parnaíba river discharge carrying terrigenous material. The HBP has an extensive drainage basin with

riparian vegetation at the flank of the rivers, several inundated areas, and swamp areas (Velloso et al., 2002). In coastal areas, the occurrence of Cyperaceae is a good indicator for salty marshlands (Behling et al., 2001) and swampy areas (Behling et al., 2001; Behling et al., 2004; Oliveira et al., 2013). The Cyperaceae pollen was the most representative pollen type within the wetland pollen group, and its relative abundance guided the general trend of this group. The wetland group reached values above 35% during MIS 4 (70 to 60 kyr) and within the several HS events of the last glacial period (Fig. 5D). The wetland group (Fig. 4) displayed higher values (~180 grains/cm³) during MIS 4 and an average higher than ~130 grains/cm³ within the HS events. Hence, despite being an anemophilous taxon with overrepresented pollen production compared to zoophilous tropical trees (Subba Reddi & Reddi, 1986), the Cyperaceae has the potential to reflect the enhancement in the Parnaíba river discharge due to its location of occurrence.

The lower values of Fe/K and Ti/Ca ratios were found between the interval of 55 kyr to 40 kyr, indicating the reduced continental contribution to the sediment core and reinforced by lower pollen concentration. For the same time interval, the percentage of the tropical dry forest pollen increased from ~9% to 28% (Fig. 5E), mainly driven by the occurrence of Asteraceae (~1% to ~10%). High relative abundance of Asteraceae may indicate selective disruption, commonly associated with disturbed or open habitats (McConnachie et al., 2011; Dingemans et al., 2014; Florenzano et al., 2015). Drier air and soil may lead plants to adjust their ecophysiological processes as vegetation cover declines, leading to less pollen production and shifts of the plant community to C4 species, shrubs, and other drought-tolerant species (Pennington et al., 2009). More sparse vegetation increases the root/shoot ratio, making the soil less stable (Boonman et al., 2019; Chen et al., 2019; Flores et al., 2020).

The lower soil stability during a prolonged dry period over the onset of MIS 3 possibly favored high erosion rates during the wet HS 5, as evident from the lower values of radiogenic εNd isotopes in the sediment core GL-1248 (de Sousa et al., 2021). The εNd isotopes are unaffected by weathering processes, and low εNd values (non-radiogenic) were indicative of erosion that revolved the oldest material and deposited it in the adjacent ocean. Despite erosion and weathering being related processes, they are not identical. Erosion indicates the removal of soil and rock materials, while weathering implicates the disintegration of rocks and minerals on Earth. During HS 5, the Ti/Ca (erosion indicator) and Fe/K (chemical weathering indicator) ratios also displayed high peaks (Fig. 5B and 5C) indicating robust load contribution of the river discharge to the adjacent ocean. The relative abundance of *Selaginella* depicted a singular rise within the HS 5 (~20%) (Fig. 5F) corroborating the reduced soil stability from ~55 to 40 kyr, as it grows on moist soil and may be used as a proxy for erosion during intense precipitation events (Behling, 2000). We suggest that the previous development of the tropical dry forest and more open landscapes was intrinsically related to lower soil stability.

Prolonged periods of rainfall do not necessarily produce considerable soil erosion if it occurs in a well-established forest (Gyssels et al., 2005), as reflected by the anti-phase pattern between the rainforest vegetation and the Fe/K ratio by the late MIS 4 and within the HS 4. The rainforest vegetation reached higher values post-HS 6 and within HS 4 events (Fig. 5G). In contrast, the wetland pollen grains and spores of S*elaginella* synchronically decayed to low values. The pollen concentration of the rainforest lowland displayed the increasing trend as opposed to the pollen concentration of tropical dry forest and wetland groups (Fig. 4). Jennerjahn et al. (2004) pointed to the increase of pollen influx post several HS events without discriminating the types of pollen used, and argued that the HS events enabled the expansion of humid forests in

NE Brazil. Our study covers a more extended period, and the results revealed no uniform responses from the lowland rainforest to different HS events. The lowland rainforest response denotes that possibly other factors may overlap the precipitation anomalies of NE Brazil.

5.2 Reconstructed vegetation in response to regional hydroclimate variability

The dominance of vegetation at a particular latitude is determined by the global temperature and moisture distribution, creating latitudinal climate zones (Kozlowski & Pallardy 1997). Today, only two ice sheets cover most of Greenland and Antarctica. However, the climate was colder during the last glacial period due to orbital forcing, and the ice sheets progressively increased. Massive sheets of ice trapped water, exposing continental shelves and lowering the absolute humidity in the atmosphere due to a reduction in both evaporation and precipitation, and generated a constrained hydrological cycle (Bush and Philander, 1998; Gasse, 2000; Muhs, 2013). The orbital forcing is thought to drive major shifts in the climate zones, potentially leading to natural fluctuations of biome boundaries (Tardif et al., 2021). Based on this, we intend to investigate how the biomes at the ecotone region of HBP rearranged over distinct conditions of global temperature and moisture distribution.

The main fluctuations in the lowland rainforest reflected in the GL-1248 record were consistent with the significant global temperature changes recorded in the Antarctic ice core (Petit et al., 1999) for the glacial period (Fig. 6A and 6B). Piacsek et al. (2021b) showed that the lowland rainforest dwindled during the last glacial period as the montane rainforest progressed, indicating global temperature as a relevant factor to the disposition of biomes in the region of HBP. However, the temperature decay of the last glacial period was not constant, with peaks in global temperature as registered in the Antarctic ice core. A warmer planet strengthens the hydrological cycle and intensifies

the moisture-holding capacity of the atmosphere (Stalg et al., 2014). Some of those abrupt warmings were followed by gains in the lowland rainforest. Before suggesting that the rise in global temperature was the main controlling factor to the rainforest lowland, we must highlight two observed patterns: 1) The opposite trend with high percentages of lowland rainforest concomitant with the drop in global temperature, as observed after the last interglacial, between 115 to 104 kyr BP. 2) A decoupling between the response of lowland rainforest and the peak of global temperature during the HS 5 event. The response of lowland rainforest during the HS 5 indicates that the rise of global temperature did not lead to positive hydrological changes in the region of HBP.

Petit et al. (1999) highlighted that the glacial-interglacial difference in temperature (ΔT) showed a frequency of orbital cycles in the 100-kyr band, followed by a 41-kyr band, while the δ^{18}Oatm which reflects changes in the global hydrological cycle, strongly imprinted the precessional frequencies (23-kyr) for the entire Vostok record. In NE Brazil, the growth phases of speleothems from Toca da Boa Vista cave (TBV; 10°11'S, 40° 58'W) were ascribed to wet periods (Wang et al. 2004). The authors correlated the growth phases of speleothems to the maximum autumn insolation (MAM), a period of high land-sea thermal contrast, improving the transport of water vapor toward the land. So far, the NE Brazil does not have another speleothems/travertine record that covers an equivalent period of time to ensure the association between the speleothem growth and the high moisture levels. However, the lowland rainforest of GL-1248 responded positively to the maximum autumn insolation (Fig. 6B and 6D), and the establishment of the lowland rainforest is recurrent in regions with dry seasons shorter than 4 months (Clapperton, 1993). High values of lowland rainforest occurred by HS 4, within MIS 4, and over part of the early glacial period

around ~110 kyr and ~80 kyr, concomitant with the maximum autumn insolation, corroborating with the high moisture levels for the region. We applied a 23 kyr bandpass filter to extract potential low-frequency components of solar and orbital signals for defining past climate variability (Fig. 6C and 6F). Thus, the precession changes should not be disregarded once it modulates austral autumn insolation at the equator and alters the incidence of heat received by the tropics, controlling the transport of humidity from ocean to land (e.g., Clement et al., 2004; Cruz et al., 2005).

Tropical dry forests include vegetation types that experience a minimum dry season of 5–7 months with strong seasonal and ecological functions such as the presence of deciduous trees and thorns (Pennington et al., 2006; Pennington et al., 2009). The onset-to-mid MIS 3 presented an increase in the percentage of the tropical dry forest despite prolonged precipitation events such as the HS 5a and HS 5. The HS 5 event occurred during the autumn insolation minimum when the transport of water vapor toward the continent was impaired. We suggest that despite being a millennial-scale event, HS 5 may have presented milder precipitation anomalies or precipitation anomalies restricted to an annual season in NE Brazil, inhibiting the development of the lowland rainforest. In this sense, we interpreted that the minimum insolation during the austral autumn has extended the dry season over NE Brazil, favoring the expansion of tropical dry forest vegetation due to the adaptive mechanisms that enable its existence in water stress conditions (Fig. 6D and 6F). Thus, the predominance of the tropical dry forest by the onset-to-mid MIS 3 suggests drier conditions than MIS 4 for NE Brazil.

Recently, the first evidence of the influence of obliquity in the NE Brazilian tropical dry forest was published (Ferreira et al., 2022). The study carried out in the watershed of the São Francisco River suggested that maximum obliquity decreased the length of the dry season to 7 months or less. According to Ferreira et al. (2022), the

maximum obliquity intensified the southeast trade winds carrying moisture from the ocean to the continent and triggering the expansion of *cerrado* tree-dominated vegetation (C3 plants) versus savanna and grassland formations (C4 plants) during the last glacial period. The length of our pollen records hampers a statistically robust detection of obliquity periodicities through time-series analyses, but the percentage of the tropical dry forest data does not seem to follow the obliquity changes (Fig. 6E and 6G). The ITCZ position strongly influences the HBP, and it is counterintuitive to infer that the further north the ITCZ is displaced, the shorter is the dry season in NE Brazil.

The increasing continental load to the Cariaco Basin (10º40.69'N, 64º58.29'W) detached by the low reflectance values, points to northward ITCZ excursions (Deplazes et al., 2013). According to Figure 6H, the percentage of the tropical dry forest of HBP follows the meridional displacement of the ITCZ during the last glacial period. The influence of the ITCZ position was also imprinted on the percentage of the tropical forest of Cariaco during the last glacial period (Fig. 6I) (Gonzalez et al., 2008; Hessler et al., 2010). The in-phase pattern between the decline in the percentage of tropical forest in the Cariaco basin and the percentage of tropical dry forest found in the GL-1248 record emphasizes the high dependence on the position of the ITCZ during the last glacial period (Fig. 6G, 6H, and 6I). However, the percentage of tropical forest in the Cariaco basin prevents further comparisons beyond the last glacial period. In contrast, the resolution achieved in the GL-1248 indicates that the 23-kyr cycle prevailed on the millennial scale over the entire record of the tropical dry forest. We suggest that the ecophysiological processes of tropical dry forests are the main factor for their development under water stress conditions across the HBP.

5.3 Succession pattern of trees in HBP

Changes in the regional hydroclimate may cause large-scale natural disturbances in vegetation cover and erosion (Whitmore, 1991; Richards, 1996). The disturbance intensity may regulate the structure and species diversity within a forest domain (Finegan, 1996). Forest patches can regenerate from the growth of pioneer trees into the development of a secondary forest (or second-growth forest) when the effects of previous disturbances are no longer evident. In the initial phases of plant succession, resource partitioning results in differential distribution of species according to their ontogeny in specific environment conditions (environmental filtering) (Wright et al., 2010; Sterck et al., 2011; Spasojevic et al., 2014). To assess the ecological succession (Gentry, 1993; Marchant et al., 2002), we removed the relative abundance of NAP pollen taxa to prevent the influence of the river flow and sea-level changes in the tropical dry forest and lowland rainforest groups. The successional pattern was ascribed to the trees and shrubs taxa of the tropical dry forest and lowland rainforest groups (Table 2).

The early life stages of plants and the pioneer trees are known better to address niche differences (Poorter, 2007). The role of functional traits in plants due to environmental conditions drives a successional gradient. For example, as the rainforest increases, it enhances its air humidity and decreases the local air temperature; a similar pattern is found in the soil moisture (Rhoades et al., 1998; Callaway, 2007), restricting the establishment of drought-adapted species. The main difference between tropical dry forests and lowland rainforests resides in the tolerance to water stress, the length of the dry season, and the evapotranspiration behavior (Clapperton, 1993). According to this definition, we applied the 23 kyr bandpass filter on both pioneer and secondary forests to better understand how the regional hydroclimate has dictated the vegetation change (Fig. 7).

Both pioneer trees (tropical dry forest and lowland rainforest) displayed greater amplitude than the secondary forests, indicating a rapid and substantial response in the initial phases of plant succession. The coupling between pioneer trees of the tropical dry forest (lowland rainforest) with the minimum (maximum) insolation of autumn (Fig. 7A and 7B) indicates that the insolation/precession may play a crucial role in the regional moisture levels, driving the pioneer phase of the successional changes in the vegetation of NE Brazil. Although the secondary rainforest lowland has displayed a good match with the 23-kyr frequencies, the secondary forests of the tropical dry forest did not show such an apparent orbital pattern and deserved a further look.

During the rainy season, dry forest trees may reduce the differences between drought deciduous and evergreen dry forest species by presenting physiological similarities (Santos et al., 2012; Apgaua et al., 2014a; Apgaua et al., 2014b; Sunderland et al., 2015). In general, the rainy season may promote the dry forest trees to show values of carbon assimilation and stomatal conductance equal to those found in rainforest trees (Van Bloem, Murphy, and Lugo, 2004). The 23-kyr cycles highlight how the regional hydroclimate variability shaped the most tree types (rainforest lowland and tropical dry forest) found in the GL-1248. However, the inadequacy of the mature tropical dry forest in the 23-kyr cycles may be related to natural temporal variations within the tree community that we were unable to account for via our temporal resolution. Though, the results also reinforce the hypothesis that other types of vegetation have possibly replaced the tropical dry forests which underwent climate changes (Pennington et al., 2000), alluding to their vulnerability.

6 Conclusions

Multi-proxy records from the marine sediment core GL-1248 retrieved off NE Brazil reveal the dynamic patterns of regional vegetation in response to the hydroclimate of the last 130 kyr. The reconstructed vegetation for NE Brazil based on pollen records has, for the first time, achieved an interglacial period beyond the Holocene. We assessed the three most representative pollen groups: wetland, lowland rainforest, and tropical dry forest. Our results showed how the vegetation distribution changed and its implications on soil erosion. The main pollen type of the wetland cluster was Cyperaceae, which displayed a coupled trend with millennial events of the last glacial period. The Cyperaceae increased during the HS and was related to vigorous discharge from the Parnaíba River. The moss fern (*Selaginella*) indicated the soil stability throughout the HS events revealing a singular soil erosion within the HS 5. The coordinated positive response between the values of Cyperaceae, *Selaginella*, and the Fe/K ratio pointed to periods with lesser soil stability across the HBP. The group of lowland rainforests displayed an anti-phase response to Cyperaceae, *Selaginella,* and the Fe/K ratio. After comparing the pollen records with the changes in terrigenous input, we suggest that the development of the tropical dry forest enhanced the soil erosion in the HBP and consequently increased the continental load to the adjacent ocean.

The lowland rainforest did not display the same gain in pollen percentage throughout the Heinrich Stadial of the last glacial period. The predominance of the tropical dry forest by the onset-to-mid MIS 3 suggested drier conditions than MIS 4 for NE Brazil. Despite the vegetation within the HBP being under the strong influence of the ITCZ position, the discrepancies in the ecophysiological processes of tropical dry forest and lowland rainforest seem to play the central role in the prevalence of each group according to changes in the length of the dry seasons. The 23-kyr bandpass

filtering ascribed greater relevance to the regional maximum autumn insolation, which dictates the ocean-continent transport of water vapor, strengthened (weakened) in maximum (minimum) insolation periods. We used the ecological definition of pioneer and secondary forest to understand the vegetation response to the hydroclimate disturbances. Only the mature tropical dry forest did not imprint the 23-kyr cycles, which may be related to physiological and structural variations within the tree community that we were unable to account for.

The reconstructed vegetation of the GL-1248 record brought light to the climatic mechanics that dictated the expansion of the tropical dry forest and lowland rainforest. The fluctuations in the relative abundance of the vegetation types over the HBP, support the hypothesis of biological radiation in the coastal route of NE Brazil and suggest the main pacing of pioneer and secondary vegetation types occurring in the 23-kyr cycles. The climate dynamics dictate the disposition of biomes that provide essential natural resources for local societies. This study highlights the vulnerability of mature dry forests and the need to improve mitigation, conservation, and adaptation strategies for NE Brazil in the face of future climate changes.

7 Acknowledgments

We thank R. Kowsmann (CENPES/Petrobras) and Petrobras Core Repository staff (Macaé/Petrobras) for providing sediment core GL-1248. Brazil National Council for the Improvement of Higher Education (CAPES) provided financial support to the first author from the. CAPES also financially supported Patricia Piacsek with a scholarship from the CAPES-ASPECTO project (Grant 88887.091731/ 2014-01). NMS acknowledges the support of CNPq (Grants 423573/2018-7; 308769/2018-0). We thank the original data generators who made their data available for future comparisons. We acknowledge the data repositories of Past Global Changes (PAGES) and the National

Oceanic and Atmospheric Administration (NOAA) that enable the paleoclimatic community to enhance their discussions.

8 References

Antonelli, A., Sanmartín I. 2011. Why are there so many plant species in the Neotropics. Taxon. 60 (2), 403-414. DOI: https://doi.org/10.1002/tax.602010.

Arz, H.W., Pätzold, J., Wefer, G., 1999. The deglacial history of the western Tropical Atlantic as inferred from high resolution stable isotope records off northeastern Brazil. Earth Planetary Science Letters. 167, 105–117. DOI: https://doi.org/10.1016/S0012-821X(99)00025-4

Apgaua, D.M.G., Coelho, P.A., Santos, R.M., Santos, P.F., Oliveira-Filho, A.T. 2014a. Tree community structure in a Seasonally Dry Tropical Forest remnant, Brazil. Cerne. 20, 173–182. DOI:10.1590/01047760.201420021540

Apgaua, D.M.G., Santos, R.M., Pereira, D.G.S., Menino, G.C.O., Pires, G.G., Fontes, M.A.L., Tng, D.Y.P. 2014b Beta-diversity in seasonally dry tropical forests (SDTF) in the Caatinga Biogeographic Domain, Brazil, and its implications for conservation. Biodiversity and Conservation. 23, 217–232. DOI:10.1007/s10531-013-0599-9

Batalha-Filho, H., Fjeldså, J., Fabre, P.-H., Miyaki, C.Y. 2013. Connections between the Atlantic and the Amazonian forest avifaunas represent distinct historical events. Journal of Ornithology. 154, 41-50. DOI: https://doi.org/10.1007/s10336-012-0866-7.

Behling, H., Arz, H.W., Pätzold, J., Wefe,r G. 2000. Late Quaternary vegetational and climate dynamics in northeastern Brazil, inferences from marine core GeoB 3104-1. Quaternary Science Reviews. 19 (10), 981-994. DOI: https://doi.org/10.1016/S0277-3791(99)00046-3.

Behling, H., Cohen, M.C.L., Lara, R.J. 2001. Studies on Holocene mangrove ecosystem dynamics of the Bragança Peninsula in northeastern Pará, Brazil. Palaeogeography, Palaeoclimatology, Palaeoecology, 167(3-4), 225–242. DOI: https://doi.org/10.1016/s0031-0182(00)00239-x

Behling, H., 2001. Late Quaternary environmental changes in the Lagoa da Curuça region (eastern Amazonia, Brazil) and evidence of Podocarpus in the Amazon lowland. Vegetation History and Archaeobotany. 10(3) 175-183. DOI: https://doi.org/10.1007/pl00006929

Behling, H., Cohen, M.C.L., Lara, R.J. 2004. Late Holocene mangrove dynamics of the Marajó Island in Amazonia, northern Brazil. Vegetation History and Archaeobotany. 13 (2), 73-80. DOI: https://doi.org/10.1007/s00334-004-0031-1.

Benninghoff, W.S. 1962. Calculation of pollen and spores density in sediments by the addition of exotic pollen in known quantities. Pollen et Spores. 4 (2), 332-333.

Berger, A., & Loutre, M-F. 1999. Parameters of the Earth's orbit for the last 5 million years in 1 kyr resolution. PANGAEA.

Blaauw, M. 2010. Methods and code for 'classical' age-modeling of radiocarbon sequences. Quaternary Geochronology. 5 (5), 12-518. DOI: https://doi.org/10.1016/j.quageo.2010.01.002.

Boonman, C.C.F., van Langevelde, F., Oliveras, I., Couédon, J., Luijken, N., Martini, D., Veenendaal, E.M. 2020. On the importance of root traits in seedlings of tropical tree species. New Phytologist. 227 (1), 156-167. DOI: https://doi.org/10.1111/nph.16370

Bouimetarhan, I., Chiessi, C.M., Gonzalez-Arango, C., Dupont, L., Voigt, I., Prange, M., Zonneveld, K. 2018. Intermittent development of forest corridors in northeastern Brazil during the last deglaciation: Climatic and ecologic evidence.

Quaternary Science Reviews. 192, 86-96. DOI: https://doi.org/10.1016/j.quascirev.2018.05.026.

Brazilian Institute of Geography and Statistics (IBGE). Maps of biomes and vegetation. Available at: <https://www.ibge.gov.br/geociencias/informacoes-ambientais/estudos-ambientais/15842-biomas.html?=&t=downloads>. (Accessed: July 13, 2022).

Broccoli, A.J., Dahl, K.A., and Stouffer, R.J. 2006. Response of the ITCZ to Northern Hemisphere cooling, Geophysical Research Letters, 33, L01702, DOI:10.1029/2005GL024546.

Burckel, P., Waelbroeck, C., Gherardi, J.M., Pichat, S., Arz, H., Lippold, H., Dokken, T., Thil, F. 2015. Atlantic Ocean circulation changes preceded millennial tropical South America rainfall events during the last glacial. Geophysical Research Letters, 42, 411-418. DOI: https://doi.org/10.1002/2014GL062512

Bush, A.B.G., Philander, S. G. H. 1998. The role of ocean–atmosphere interactions in tropical cooling during the last glacial maximum. Science, 279, 1341–1344. DOI:10.1126/science.279.5355.134

Callaway, R.M. 2007. Positive Interactions and Interdependence in Plant Communities. Dordrecht. Springer.

Cárdenas, M.L., Gosling, W. D., Sherlock, S. C., Poole, I., Pennington, R. T., Mothes P. 2011. The response of vegetation on the Andean flank in western Amazonia to Pleistocene climate change. Science. 331, 1055-1058. DOI: 10.1126/science.1197947

Castro, A.A.J.F., Martins, F.R., Fernandes, A.G. 1998. The woody flora of cerrado vegetation in the state of Piaui, northeastern Brazil. Edinburgh Journal of Botany. 55(03), 455. DOI: https://doi:10.1017/s0960428600003292.

Chen, G., Hobbie, S., Reich, P.B., Yang, Y., Robinson, D. 2019. Allometry of fine roots in forest ecosystems. Ecology Letters. 22, 322-331. DOI: https://doi.org/10.1111/ele.13193

Clapperton, C.M. 1993. Nature of environmental changes in South America at the Last Glacial Maximum. Palaeogeography, Palaeoclimatology, Palaeoecology, 101 (3-4), 189-208. DOI: https://doi.org/10.1016/0031-0182(93)90012-8.

Clement, A.C., Hall, A., Broccoli, A.J. 2004. The importance of precessional signals in the tropical climate. Climate Dynamics. 22 (4), 327-341. DOI: https://doi.org/10.1007/s00382-003-0375-8.

Climate Change Knowledge Portal (CCKP). 2021. "Climate projections › CMIP5 data", available at: <https:// https://climateknowledgeportal.worldbank.org/download-data>. (accessed July 13, 2022)

Cohen, M.C.L., Rossetti, D.F., Pessenda, L.C.R., Friaes, Y.S., Oliveira, P.E. 2014. Late Pleistocene glacial forest of Humaita, western Amazonia. Palaeogeography Palaeoclimatology Palaeoecology, 415, 37-47. DOI: https://doi.org/10.1016/j.palaeo.2013.

Cole, M.M. 1986. The Savannas. Academic Press London 438 pp.

Colinvaux, P.A., de Oliveira, P.E., Moreno, J.E., Miller, M.C., Bush, M.B. 1996. A long pollen record from lowland Amazonia, forest and cooling in glacial times. Science. 274, 85-88. DOI: http://doi.org/10.1126/science.274.5284.85.

Correia Filho, W.L.F., Oliveira-Júnior, J.F., Santiago, D.B., Terassi, P.M.B., Teodoro, P.E., Gois, G., Blanco, C.J.C., Souza, P.H.A., Costa, M., Santos P.J. 2019. Rainfall variability in the Brazilian northeast biomes and their interactions with meteorological systems and ENSO via CHELSA product. Big Earth Data, 3, 315-337. DOI: https://doi.org/10.1080/20964471.2019.1692298

Costa, L.P. 2003. The historical bridge between the Amazon and the Atlantic Forest of Brazil: a study of molecular phylogeography with small mammals. Journal of Biogeography. 30(1), 71-86. DOI: https:// doi:10.1046/j.1365-2699.2003.00792.x.

Cruz, F.W., Burns, S.J., Karmann, I., Sharp, W.D., Vuille, M., Cardoso, A.O., Ferrari, J.A., Dias, P.L.S., Viana, Jr.O. 2005. Insolation-driven changes in atmospheric circulation over the past 116,000 years in subtropical Brazil. Nature. 434, 63–66. DOI: https://doi.org/10.1038/nature03365

Davis M.B., Deevey E.S. 1964. Pollen accumulation rates: estimates from Late-Glacial sediment Rogers Lake. Science. 145, 1293—95

de Oliveira, P.E., Barreto, A.M.F., Suguio, K. 1999. Late Pleistocene/Holocene Climatic and Vegetational history of the Brazilian caatinga: the fossil dunes of the middle Sao Francisco River. Paleogeography, Paleoclimatology, Paleoecology. 152, 319-337. DOI: https://doi.org/10.1016/S0031-0182(99)00061-9

de Sousa, T.A., Venancio, I.M., Valeriano, C.d.M., Heilbron, M., Carneiro, W. D., Mane, M.A., de Almeida, J.C. H., Omoak, J.M., Albuquerque, A.L.S., Silva-Filho, E. V. 2021. Changes in Sedimentary Provenance and Climate off the Coast of Northeast Brazil since the Last Interglacial. Marine Geology. 435, 106454. DOI:10.1016/j.margeo.2021.106454

Deplazes, G., Lückge, A., Peterson, L.C., Timmermann, A., Hamann, Y., Hughen, K.A., Röhl, U., Laj, C., Cane, M.A., Sigman, D.M., Haug, G.H. 2013. Links between tropical rainfall and North Atlantic climate during the last glacial period. Nature Geoscience. 6, 213-217. DOI: https://doi.org/10.1038/ngeo1712.

Dingemans, T., Mensing, S.A., Feakins, S.J., Kirby, M.E., Zimmerman, S.R.H. 2014. 3000 years of environmental change at Zaca Lake, California, USA. Frontiers in Ecology and Evolution, 2.34. doi: 10.3389/fevo.2014.00034

Dupont, L.M., Schlütz, F., Ewah, C.T., Jennerjahn, T.C., Paul, A., Behling, H. 2010. Two-step vegetation response to enhanced precipitation in Northeast Brazil during Heinrich Event 1. Global Change Biology. 16 (6), 1647-1660. DOI: https://doi.org/10.1111/j.1365-2486.2009.02023.x.

Fadina, O.A., Venancio, I.M., Belem, A., Silveira, C.S., Bertagnolli, D.d.C., Silva-Filho, E.V., Albuquerque, A.L.S. 2019. Paleoclimatic Controls on Mercury Deposition in Northeast Brazil since the Last Interglacial. Quaternary Science Reviews. 221, 105869. DOI:10.1016/j.quascirev.2019.105869

Faegri, K., Iversen, J. 1989. Textbook of pollen analysis (4th edition). Revised by K. Faegri P.E. Kaland & K. Krzywinski. John Wiley and Sons (Chichester).

Ferreira, J.Q., Chiessi, C.M., Hirota, M., Oliveira, R.S., Prange, M., Haggi, C.S., Crivellari, C., Nandini-Weiss, S.D., Bertassoli Jr.D.J., Campos, M.C., Mulitza, S., Albuquerque, A.L.S., Bahr, A., Schefuß, E. 2022. Changes in obliquity drive tree cover shifts in eastern tropical South America. Quaternary Science Reviews. 279, 107402. DOI:https://doi.org/10.1016/j.quascirev.2022.107402

Finegan, B. 1966. Pattern and process in neotropical secondary rain forests: The first 100 years of succession. Trends in Ecology & Evolution, 11(3). 119-24. DOI: 10.1016/0169-5347(96)81090-1

Florenzano, A, Marignani, M., Rosati, L., Fascetti, S., Mercuri, A.M. 2015. Are Cichorieae an indicator of open habitats and pastoralism in current and past vegetation studies? Blant Biosystems. 149,154–165. DOI: https://doi.org/10.1080/11263504.2014.998311

Flores, B. M., Staal, A., Jakovac, C. C., Hirota, M., Holmgren, M., Oliveira, R. S. 2019. Soil erosion as a resilience drain in disturbed tropical forests. Plant and Soil. 450, 11-25. DOI:10.1007/s11104-019-04097-8

Gasse, F. 2000. Hydrological changes in the African tropics since the Last Glacial Maximum. Quaternary Science Reviews, 19, 189–211. DOI: 10.1016/S0277-3791(99)00061-X

González, C., Dupont, L. M., Behling, H., Wefer, G. 2008. Neotropical vegetation response to rapid climate changes during the last glacial period: Palynological evidence from the Cariaco Basin. Quaternary Research. 69(2), 217-230. DOI: https://doi.org/10.1016/j.yqres.2007.12.00.

Gentry, A.H. 1993. Woody plants of northwest South America. Conservation International, Washington, DC.

Govin, A., Holzwarth, U., Heslop, D., Ford, K L., Zabel, M., Mulitza, S., Collins, J.A., Chiessi, C.M. 2012. Distribution of major elements in Atlantic surface sediments (36°N-49°S): Imprint of terrigenous input and continental weathering. Geochemistry, Geophysics, Geosystems. 13 (1), 1-23. DOI: https://doi.org/10.1029/2011GC003785.

Gyssels, G., Poesen, J., Bochet, E., Li, Y. 2005. Impact of plant roots on the resistance of soils to erosion by water: a review. Progress in Physical Geography. 29 (2), 189-217. DOI: https://doi.org/10.1191/0309133305pp443ra.

Hemming, S.R. 2004. Heinrich events: Massive late Pleistocene detritus layers of the North Atlantic and their global climate imprint. Reviews Geophysics. 42(1). DOI: https://doi.org/10.1029/2003RG000128

Hermanowski, B., da Costa, M.L., Carvalho, A.T., Behling, H. 2012. Palaeoenvironmental dynamics and underlying climatic changes in southeast Amazonia (Serra Sul dos Carajás, Brazil) during the late Pleistocene and Holocene. Palaeogeography, Palaeoclimatology, Palaeoecology, 365-366, 227-246. DOI: 617 https://doi.org/10.1016/j.palaeo.2012.09.030.

Hessler, I., Dupont, L., Bonnefille, R., Behling, H., González, C., Helmens, K.F., Hooghiemstra, H., Lebamba, J., Ledru, M-P., Lézine, A-M., Maley, J., Marret, F., Vincens, A. 2010. Millennial-scale changes in vegetation records from tropical Africa and South America during the last glacial. Quaternary Science Reviews, 29(21-22), 2882-2899. DOI:10.1016/j.quascirev.2009.11.029

Hoorn, C. Wesselinghh, F.P., Steegem, T., Bermudeza, A., Mora, Sevink, J., Sanmartín, I. Sanchez-Meseguer, A., Anderson, C.L.J., Figueiredo, P., Jaramillo, C., Riff, D., Negri, F.R., Hooghiemstra, H., Lundberg, J., Stadler, T., Särkinenan, T., Antonelli, D.A. 2010. Amazonia Through Time: Andean Uplift, Climate Change, Landscape Evolution, and Biodiversity. Science. 330, 927. DOI: 10.1126/science.1194585

Jennerjahn, T.C., Ittekkot, V., Arz, H.W., Behling, H., Pätzold, J. Wefer, G. 2004. Asynchronous terrestrial and marine signals of climate change during Heinrich Events. Science. 306 (5705), 2236-2239. DOI: https://doi.org/10.1126/science.1102490.

Johns, W.E., Lee, T.N., Beardsley, R.C., Candela, J., Limeburner, R., Castro, B. 1998. Annual cycle and variability of the North Brazil Current. Journal of Physical Oceanography. 28 (1), 103-128. DOI: https://doi.org/10.1175/1520-0485(1998)028<0103:ACAVOT>2.0.CO;2.

Kozlowski, T.T., Pallardy, S.G. 1997. Growth Control in Woody Plants. Academic Press, San Diego, CA.

Kuhlmann, K. 1977. "Der Thron im alten Ägypten: Untersuchungen zu Semantik, Ikonographie und Symbolik eines Herrschaftszeicchens." Gluckstadt:J.J. Augistin.

Laskar, J., Robutel, P., Joutel, F., Gastineau, M., Correia, A.C.M., Levrard, B. 2004. A long term numerical solution for the insolation quantities of the Earth. Astronomy & Astrophysics. 428, 261-285.

Ledo, R.M.D., Colli, G.R. 2017. The historical connections between the Amazon and the Atlantic Forest revisited. Journal of Biogeography. 44 (11), 2551-2563. DOI: https://doi.org/10.1111/jbi.13049.

Ledru, M.-P., Mourguiart, P., Ceccantini, G., Turcq, B., Sifeddine, A. 2002. Tropical climates in the game of two hemispheres revealed by abrupt climatic change. Geology, 30, 275-278. DOI: https://doi.org/10.1130/0091-7613(2002)030<0275:TCITGO>2.0.CO;2

Li, M., Hinnov, L., Kump, L. 2019. Acycle: Time-series analysis software for paleoclimate research and education. Computers & Geosciences 127, 12-22. Doi: https://doi.org/10.1016/j.cageo.2019.02.011

Lima, A.G.M., de Melo A.M.B.L. 1985. Atlas Geográfico do Estado da Paraíba. Relevo. In Secretária da Educação; Governo do Estado da Paraíba; Universidade Federal da Paraíba. João Pessoa (PB): Grafset. p.26-29.

Maher, L.J.J. 1972. Nomogram for computing 0.95 confidence limits of pollen data. Review of Paleobotany and Palynology 13, 85-93.

Maher, L.J.J. 1981. Statistics for microfossil concentration measurements employing samples spiked with marker grains. Review Palaeobotany and Palynology 32, 153-191.

Marchant, R., Almeida, L., Behling, H., Berrio, J.C., Bush, M., Cleef, A., Duivenvoorden, J., Kappelle, M., de Oliveira, P., de Oliveira-Filho, A.T., Lozano-Garcia, S., Hooghiemstra, H., Ledru, M.-P., Ludlow-Wiechers, B., Markgraf, V., Mancini, V., Paez, M., Preto, A., Rangel, O., Salgado-Labouriau, M.L. 2002. Distribution and ecology of parent pollen lodged within the Latin American Pollen Database. Review of Palaeobotany and Palynology. 121, 1-75. DOI: 10.1016/S0034-6667(02)00082-9

McConnachie, A.J., Strathie, L.W., Mersie, W., Gebrehiwot, L., Zewdie, K., Abdurehim, A., Abrha, B., Araya, T., Asaregew, F., Assefa, F., Gebre-Tsadik, R., Nigatu, L., Tadesse, B., Tana, T. 2011. Current and potential geographical distribution of the invasive plant Parthenium hysterophorus (Asteraceae) in eastern and southern Africa. Weed Research. 51(1):71–84. doi: 10.1111/j.1365-3180.2010.00820.x

McGee, D., Moreno-Chamarro, E., Green, B., Marshall, J., Galbraith, E., Bradtmiller, L. 2018. Hemispherically asymmetric trade wind changes as signatures of past ITCZ shifts, Quaternary Science Reviews, 180, 214-228, ISSN 0277-3791. DOI: https://doi.org/10.1016/j.quascirev.2017.11.020

Mulitza, S., Prange, M., Stuut, J.-B., Zabel, M., Dobeneck, T. von, Itambi, A.C., Nizou, J., Schulz, M., Wefer, G. 2008. Sahel megadroughts triggered by glacial slowdowns of Atlantic meridional overturning. Paleoceanography, 23, p. PA4206.

Mulitza, S., Chiessi, C.M., Schefuß, E., Lippold, J., Wichmann, D., Antz, B., Mackensen, A., Pau, A., Prange, M., Rehfeld, K., Werner, M., Bickert, T., Frank, N., Kuhnert, H., Lynch stieglitz J., Portilho Ramos, R.C., Sawakuchi, AO., Schulz, M., Schwenk, T., Tiedemann, R., Vahlenkamp, M., Zhang, Y. 2017. Synchronous and proportional deglacial changes in Atlantic meridional overturning and northeast Brazilian precipitation. Paleoceanography. 32, 622-633. DOI: https://doi.org/10.1002/2017PA003084.

Muhs, D.R. 2013. The geologic records of dust in the Quaternary. Aeolian Research. Volume 9, Pages 3-48, ISSN 1875-9637, DOI: https://doi.org/10.1016/j.aeolia.2012.08.001.

Nace, T.E., Baker, P.A., Dwyer, G.S., Silva, C.G., Rigsby, C.A., Burns, S.J., Giosan, L., Otto-Bliesner, B., Liu, Z., Zhu, J. 2014. The role of North Brazil Current transport in the paleoclimate of the Brazilian Nordeste margin and paleoceanography of

the western tropical Atlantic during the late Quaternary. Palaeogeography, Palaeoclimatology, Palaeoecology. 415, 3-13. DOI: https://doi.org/10.1016/j.palaeo.2014.05.030.

North Greenland Ice Core Project members. 2004. High-resolution record of Northern Hemisphere climate extending into the last interglacial period. Nature 431(7005):147-151.

Oliveira, R., Silva, A., Ribeiro, A., Araújo, J., Oliveira, O., Camacho, R. 2013. List of angiosperm species of the riparian vegetation of the Apodi-Mossoró River, Rio Grande do Norte, Brazil. Check List. 9 (4), 740-751. DOI: https://doi.org/10.15560/9.4.740.

Pennington, R.T., Prado, D.E., Pendry, C.A. 2000. Neotropical seasonally dry forests and Quaternary vegetation changes. Journal of Biogeography. 27, 261–273. DOI:10.1046/j.1365-2699.2000.00397.x

Pennington, R.T., Lewis, G.P., Ratter, J.A. 2006. An overview of the plant diversity, biogeography and conservation of neotropical savannas and seasonally dry forests. In: Pennington RT, Lewis GP, Ratter JA, editors. Neotropical Savannas and Seasonally Dry Forests: Plant Diversity, Biogeography, and Conservation. Boca Raton, FL: CRC Press; pp. 1–29.

Pennington, R.T., Lavin, M., Oliveira–Filho, A. 2009. Woody plant diversity, evolution and ecology in the tropics: Perspectives from seasonally dry tropical forests. Annual Review of Ecology, Evolution, and Systematics. 40:437–457. DOI: https://doi.org/10.1146/annurev.ecolsys.110308.120327

Petit, J.R., Jouzel, J., Raynaud, D., Barkov, N.I., Barnola, J.-M., Basile, I., Bender, M., Chappellaz, J., Davis, M., Delaygue, G., Delmotte, M., Kotlyakov, V.M., Legrand, M., Lipenkov, V.Y., Lorius, C., P´epin, L., Ritz, C., Saltzman, E., Stievenard, M. 1999.

Climate and atmospheric history of the past 420000 years from the Vostok ice core, Antarctica. Nature. 399, 429–436. DOI: https://doi.org/10.1038/20859.

Piacsek, P., Behling, H., Gu, F., Venancio, I. M., Lessa, D.V.O., Belem, A., Albuquerque, A.L.S. 2021a. Changes in sea surface hydrography and productivity in the western equatorial Atlantic since the Last Interglacial. Palaeogeography, Palaeoclimatology, Palaeoecology. DOI: 10 1016 /j palaeo 2020 109952

Piacsek, P., Behling, H., Venancio, I. M., Ballalai, J. M., Nogueira, J., Albuquerque, A.L.S. 2021b. Reconstruction of vegetation and low latitude ocean-atmosphere dynamics of the past 130 kyr, based on south American montane pollen types. Global and Planetary Change. DOI: 10.1016/j.gloplacha.2021.103477

Pinaya, J.L.D., Cruz, F.W., Ceccantini, G.C.T., Pedro, L.P, Corrêa Pitman, N., Vemado, F., Lopez, S.M.A., Pereira, Filho A.J., Grohmann, C.H., Chiessi C.M., Stríkis, N.M., Horák-Terra, I., Pinaya, W.H.L., De Medeiros, V.B., Santos, R. De A., Akabane, T.K., Silva, M.A., Cheddadi, R., Bush, M., Henrot, J., François, L., Hambuckers, A., Boye, F., Carré, M., Coissac, E., Faccola, F., Huang, K., Lézine, A-M., Nourelbait, M., Rhoujjati, A., Taberlet, P., Sarmiento, F., Abel-Schaad, D., Alba-Sánchez, F., Zheng, Z., de Oliveira, P.E. 2019. Brazilian montane rainforest expansion induced by Heinrich stadial 1 event. Scientific Reports. 9 (17912). DOI: https://doi.org/10.1038/s41598-019-53036-1.

Poorter, L. 2007. Are species adapted to their regeneration niche, adult niche, or both? The American Naturalist., 169, 433–442.

Por, F.D. 1992. Sooretama: the Atlantic rain forest of Brazil. SPB Academic Publishing. The Hague, p. 130.

Tardif, D., Toumoulin, A., Fluteau, F., Donnadieu, Y., Le Hir, G., Barbolini, N., Licht, A., Ladant, J.B., Sepulchre, P. Viovy, N., Hoorn, C., Dupont-Nivet, G. 2021.

Orbital variations as a major driver of climate and biome distribution during the greenhouse to icehouse transition. Science Advances 7(43):eabh2819. DOI: 10.1126/sciadv.abh2819.

Reimer, P.J., Bard, E., Bayliss, A., Beck, J.W., Blackwell, P.G., Ramsey, C.B., Buck, C.E., Cheng, H., Edwards, R.L., Friedrich, M., Grootes, P.M., Guilderson, T.P., Haflidason, H., Hajdas, I., Hatté, C., Heaton, T.J., Hoffmann, D.L., Hogg, A.G., Hughen, K.A., Kaiser, K.F., Kromer, B., Manning, S.W., Niu, M., Reimer, R.W., Richards, D.A., Scott, E.M. Southon, J.R., Staff, R.A., Turney, C.S.M., Van Der Plicht, J. 2013. Int. Cal13 and Marine13 radiocarbon age calibration curves 0-50,000 years cal BP. Radiocarbon. 55 (04), 1869-1887. DOI: https://doi.org/10.2458/azu_js_rc.55.16947.

Rhoades, C.C., Eckert, G. E., Coleman, D.C. 1998. Effect of pasture trees on soil nitrogen and organic matter: implications for tropical montane forest restoration. Restoration Ecology. 6, 262–270. DOI: 10.1046/j.1526-100X.1998.00639.x

Rühlemann, C., Frank, M., Hale, W., Mangini, A., Mulitza, S., Muller, P.J., Wefer, G. 1996. Late Quaternary productivity changes in the western equatorial Atlantic: evidence from 230Th-normalized carbonate and organic carbon accumulation rates. Marine Geology. 135 (1–4), 127–152. https://doi.org/10.1016/S0025-3227(96)00048-5.

Santos, R.M., Oliveira-Filho, A.T., Eisenlohr, P.V., Queiroz, L.P., Cardoso, D.B., Rodal, M.J.N. 2012. Identity and relationships of the Arboreal Caatinga among other floristic units of seasonally dry tropical forests (SDTFs) of north-eastern and central Brazil. Ecology and Evolution. 2, 409–428. doi:10.1002/ece3.91

Shimizu, M.H., Anochi, J.A. Kayano, M.T. 2022. Precipitation patterns over northern Brazil basins: climatology, trends, and associated mechanisms. Theoretical and Applied Climatology. 147, 767–783. DOI: https://doi.org/10.1007/s00704-021-03841-4

Silveira, M.H.B., Mascarenhas, R., Cardoso, D., Batalha-Filho, H. 2019. Pleistocene Climatic Instability Drove the Historical Distribution of Forest Islands in the Northeastern Brazilian Atlantic Forest. Palaeogeography, Palaeoclimatology, Palaeoecology. 527, 67-76. DOI: https://doi.org/10.1016/j.palaeo.2019.04.028.

Spasojevic, M.J., Yablon, E.A., Oberle, B., Myers J.A. 2014. Ontogenetic trait variation influences tree community assembly across environmental gradients. Ecosphere, 5(10), 1-20.

Sterck, F., Markesteijn, L., Schieving, F., Poorter L. 2011. Functional traits determine trade-offs and niches in a tropical forest community. Proceedings of the National Academy of Sciences, 108(51), 20627-20632. DOI: 10.1073/pnas.1106950108

Stockmarr, J. 1971. Tablets with spores used in absolute pollen analysis. Pollen et Spores. 13(4), 615-621.

Stramma, L., Fischer, J., Reppin, J. 1995. The North Brazil Undercurrent. Deep-Sea Research I. 42 (5), 773-795. DOI: https://doi.org/10.1016/0967-0637(95)00014-W

Stríkis, N.M., Cruz, F.W., Barreto, E.A.S., Naughton, F., Vuille, M., Cheng, H., Voelker, A.H.L., Zhang, H., Karmann, I., Edwards, L., Auler, AS., Santos, R.V., Sales, H.R. 2018. South American monsoon response to iceberg discharge in the North Atlantic. The Proceedings of the National Academy of Sciences. 115 (15), 3788-3793. DOI: https://doi.org/10.1073/pnas.1717784115.

Subba Reddi, C., Reddi, N.S. 1986. Pollen production in some anemophilous angiosperms. Grana. 25 (1), 55-61. DOI: https://doi.org/10.1080/00173138609429933.

Sunderland, T., Apgaua, D., Baldauf, C., Blackie, R., Colfer, C., Cunningham, A.B., Dexter, K., Djoudi, H., Gautier, D., Gumbo, D., Ickowitz, A., Kassa, H., Parthasarathy, N., Pennington, R.T., Paumgarten, F., Pulla, S., Sola, P., Tng, D.Y.P., Waeber, O.,

Wilmé, L. 2015. Global dry forests: a prologue. International Forestry Review. 17(S2), 1–9. DOI:10.1505/146554815815834813

Utida, G., Cruz, F.W., Etourneau, J., Bouloubassi, I., Schefuß, E., Vuille, M., Novello, V.F., Prado, L.F., Sifeddine, A., Klein, V., Zular, A., Viana, J.C.C., Turcq, B. 2009. Tropical South Atlantic influence on northeastern Brazil precipitation and ITCZ displacement during the past 2300 years. Scientific Reports. 9 (1698). DOI: https://doi.org/10.1038/s41598-018-38003-6.

Van Bloem, S.J., Murphy, P.G., Lugo, A.E. 2004. TROPICAL FORESTS. Tropical Dry Forests. Encyclopedia of Forest Sciences, Pages 1767-1775, ISBN 9780121451608. DOI: https://doi.org/10.1016/B0-12-145160-7/00176-9.

Velloso, A.L., Sampaio, E.V.S.B., Pareyn, F.C.C. 2002. Ecorregiões propostas para o Bioma caatinga. In: Recife, Associação Plantas do Nordeste. The Nature Conservancy do Brasil, Instituto de Conservaçˆao Ambiental (76pp.).

Venancio, I.M., Mulitza, S., Gevin, A., Santos, T.P., Lessa, D.O., Albuquerque, A.L.S., Chiessi, C.M., Tiedemann, R., Vahlenkamp, M., Bitcket, T., Schulz, M. 2018. Millennial- to orbital-scale responses of western equatorial Atlantic thermocline depth to changes in the trade wind system since the Last Interglacial. Paleoceanography and Paleoclimatology. 33 (12), 1490-1507. DOI: https://doi.org/10.1029/2018PA003437.

Waelbroek, C., Labeyrie, L., Michel, E., Duplessy, J.C., McManus, J.F., Lambeck, K., Labracherie, M. 2002. Sea-level and deep water temperature changes derived from benthic foraminifera isotopic records. Quaternary Science Reviews. 21 (1–3), 295–305.

Wang, X., Auler, A.S., Edwards, R.L., Cheng, H., Cristalli, P.S., Smart, P.L., Richards, D.A., Shen, C-C. 2004. Wet periods in northeastern Brazil over the past 210 kyr linked to distant climate anomalies. Nature. 432 (7018), 740-743. DOI: https://doi.org/10.1038/nature03067

Whitmore, T.C. 1991. Tropical rain forest dynamics and its implications for management. Rain Forest Regeneration and Management (eds. A. Gómez-Pompa, T.C. Whitmore & M., Hadley), pp. 67–89. Parthenon Publishing, Lancaster, UK, and UNESCO, Paris.

Wright, S.J., Kitajima, K., Kraft, N.J., Reich, P.B., Wright, I.J., Bunker, D.E., Engelbrecht, B.M. 2010. Functional traits and the growth-mortality trade-off in tropical trees. Ecology, 91(12), 3664-3674. DOI: https://doi.org/10.1890/09-2335.1

Zhang, Y., Chiessi, C.M., Mulitza, S., Zabel, M., Trindade, R.I.F., Hollanda, M.H.B.M., Dantas, E.L., Govin, A., Tiedemann, R., Wefer, G. 2015. Origin of increased terrigenous supply to the NE South American continental margin during Heinrich Stadial 1 and the Younger Dryas. Earth Planetary Science Letters. 432, 493-500. DOI: https://doi.org/10.1016/j.epsl.2015.09.054.

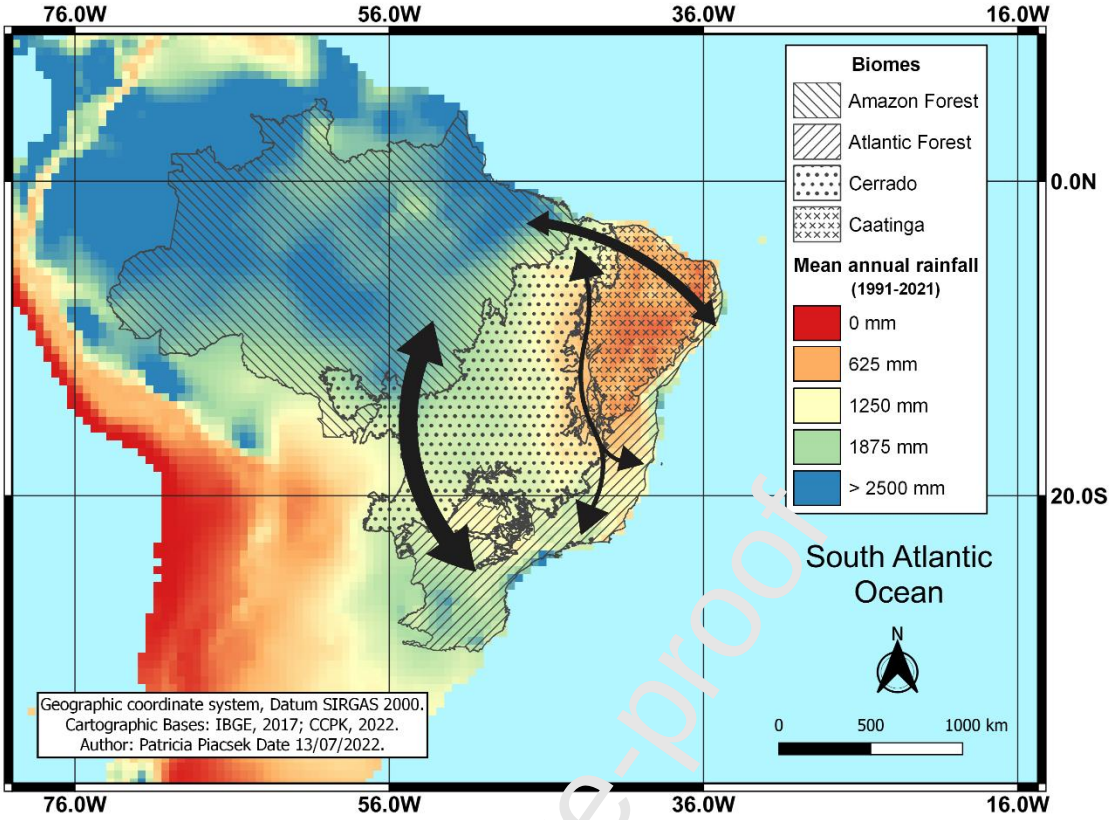

Figure 1: Map of the mean annual rainfall from 1991 to 2021 (CCKP, 2022) and the disposition of the modern terrestrial biomes discussed in this paper (IBGE, 2014). The black arrows illustrate the main routes of biotic interchange between the Amazon and the Atlantic rainforest (Por, 1992). The thickness of the arrows is related to the importance of the route. The map also shows the rainfall variability of biomes in NE Brazil from 1979 to 2013: Amazon rainforest (1847.9 mm ± 418.7 mm), *caatinga* (773.1 mm ± 212.5 mm), and *cerrado* (1196.6 mm ± 218.9 mm), Atlantic rainforest (1363.8 mm ± 217.0 mm) (Correia Filho *et al.*, 2019).

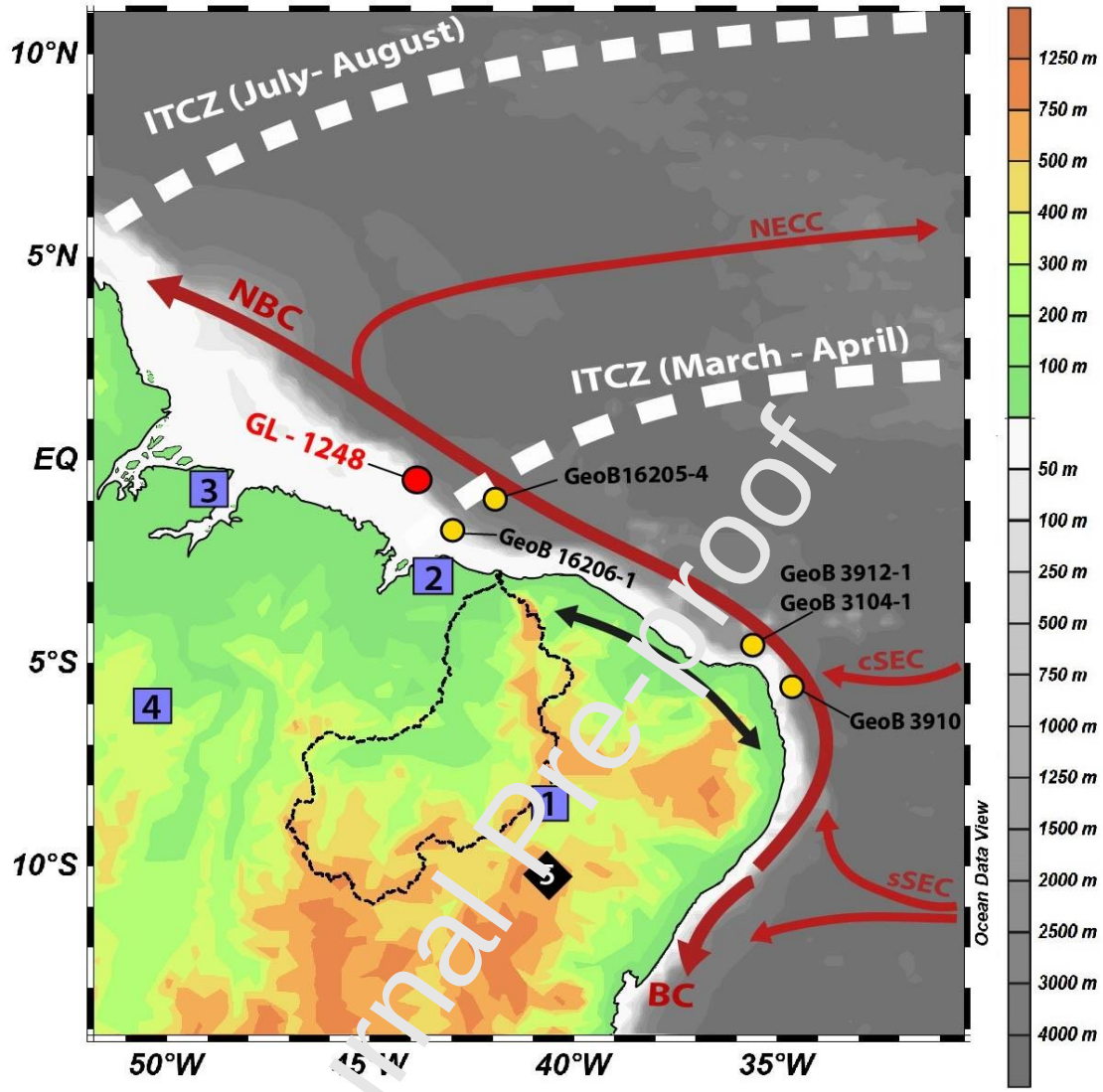

Figure 2: Topographical map of the study area. The red dot marks the location of the studied marine core GL-1248 (0° 55.2'S, 43° 24.1'W). The location of the previous marine sediment cores GeoB 16206-1 (Zhang *et al.*, 2015), GeoB 16205-4 (Bouimetarhan *et al*, 2018); GeoB 3912-1/GeoB 3104-1 (Behling *et al.*, 2000; Jennerjahn *et al.*, 2004), and GeoB 3910-2 (Dupont *et al.*, 2010) are shown by the yellow dots. The blues squares show the location of the palynological records covering the Holocene and the last glacial: 1) Icatu River peat-bog, (De Oliveira *et al.*, 1999); 2) MA97-1, (Ledru *et al.*, 2002); 3) Barra Velha, at Marajó Island, (Behling *et al.*, 2004); 4) Pántano de Maurítia, (Hermanowski *et al.*, 2012); 5) The location of the speleothem record from Toca da Boa Vista (Wang *et al.*, 2004) is indicated by the black diamond. The red arrows on the Atlantic Ocean represent the warm surface currents North Equatorial Countercurrent (NECC), North Brazil Current (NBC), South Equatorial Current with central and southern branches (cSEC, and sSEC), and Brazil Current (BC). The white dashed line displays the southernmost position of the Intertropical Convergence Zone (ITCZ) during the end of Austral autumn (March-April) and the Austral winter (July-August). The black both sides' arrow indicates the location for the possibility to form coastal forest corridors connecting Amazonian and Atlantic rainforests through the coastal route of NE Brazil. The dashed line shows the hydrographical basin of the Parnaiba (~344 km^2) in NE Brazil.

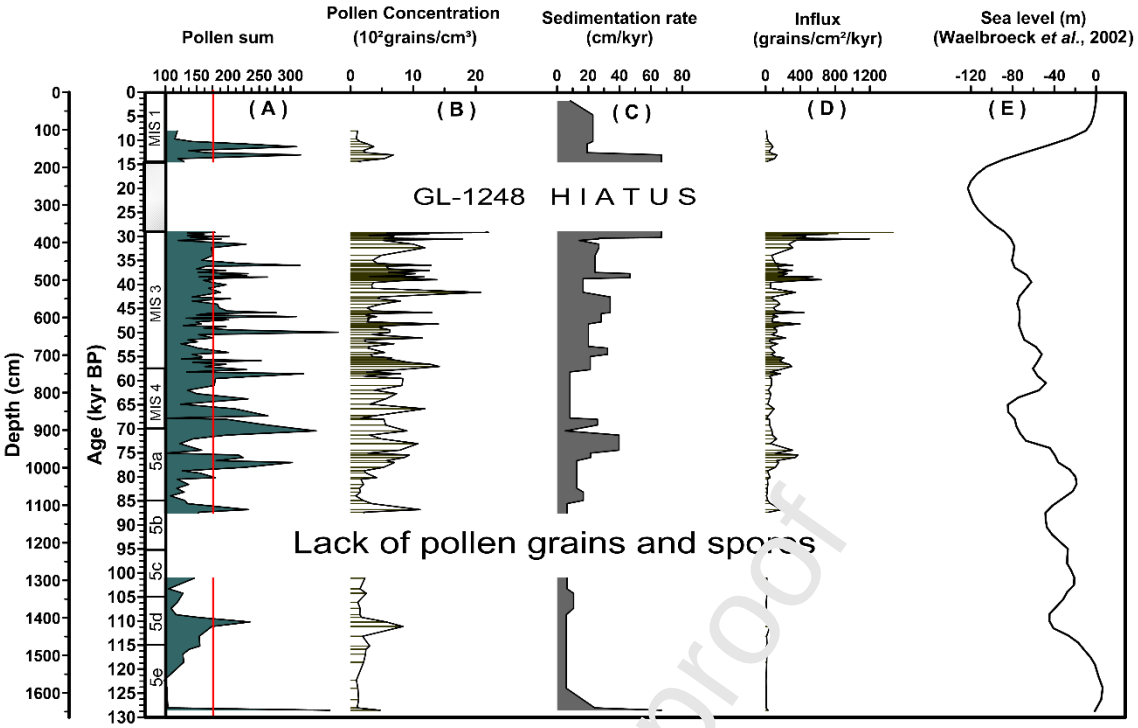

Figure 3: (A) Pollen sum, the red line indicates the average of the sum of pollen and spores; (B) Pollen concentration (10^agrains/cm³); (C) GL-1248 Sedimentation rate (cm/kyr) (Venancio *et al.*, 2018); (D) Pollen influx (10^agrains/cm²/kyr); (E) Sea Level (m) (Waelbroeck *et al.*, 2002).

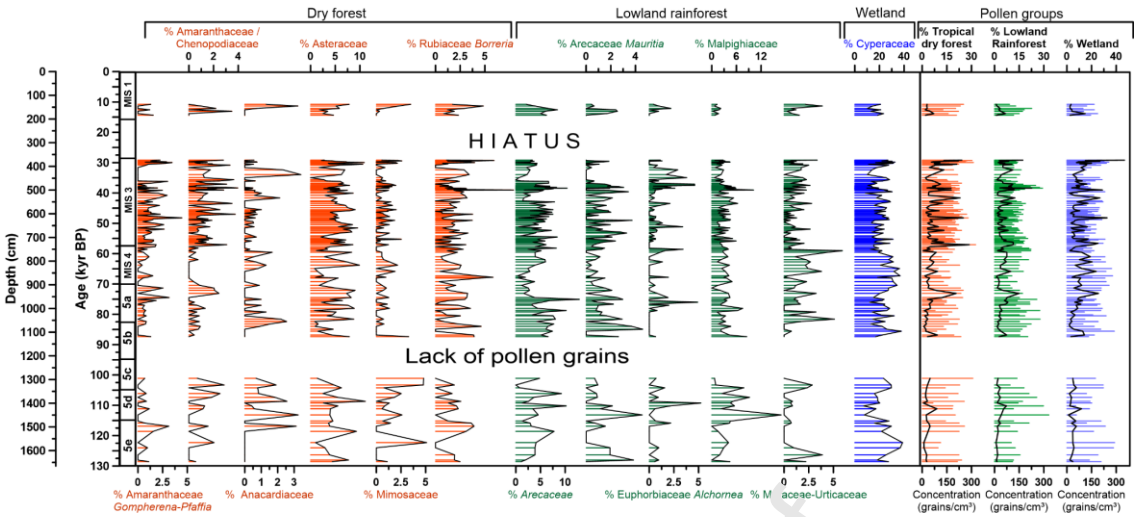

Figure 4: Chart of the relative abundance of 12 pollen types of main groups of taxa (tropical dry forest, lowland rainforest, and wetland) along the marine core GL-1248. The total percentage of each pollen group (tropical dry forest, lowland rainforest, and wetland) are displayed on the right and the black line is related to their respective pollen concentrations. The pollen data of GL-1248 were previously addressed in Piacsek *et al.* (2021b).

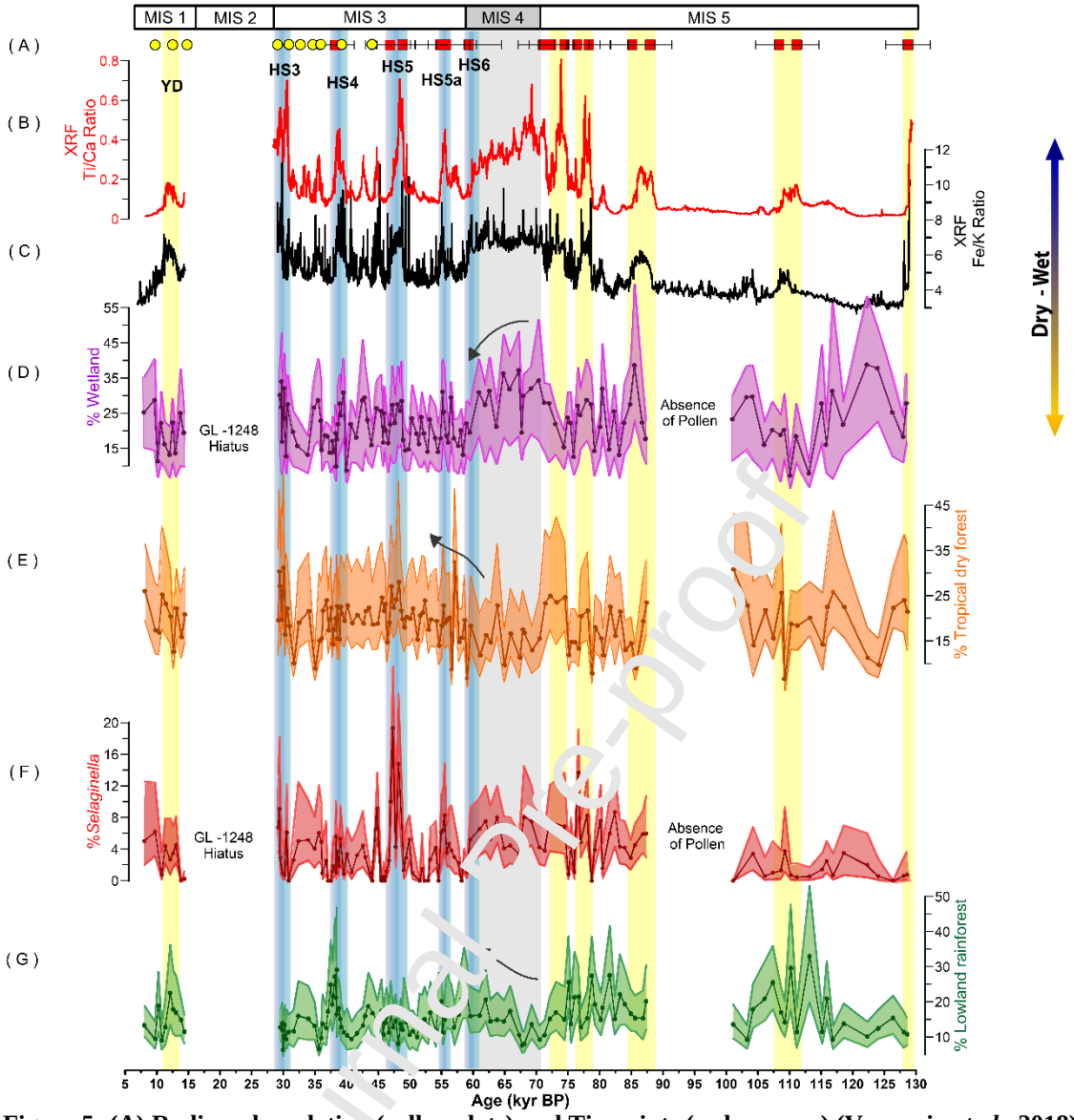

Figure 5: (A) Radiocarbon dating (yellow dots) and Tie-points (red squares) (Venancio *et al.*, 2018); (B) X-ray fluorescence (XRF) Ti/Ca ratio of the GL-1248 core (Venancio *et al.*, 2018); (C) XRF Fe/K ratio of GL-1248 (de Sousa *et al.*, 2021); (D) %Wetland group; (E) %Tropical dry forest group; (F) *Selaginella* spores; (G) %Lowland rainforest group; Shadings indicate the 95% confidence interval calculated after Maher (1972). The double-headed arrow indicates the transition from dry to wet, related to the Ti/Ca, Fe/K and wetland taxa. The Heinrich Stadials (HS) are marked in light blue, with the respective acronyms. The MIS 4 is marked in gray, the Younger Dryas (YD) and the other Stadials of the Early glacial (~70 - 115 kyr) and the last interglacial (MIS5e, ~115 -130 kyr) are highlighted in yellow.

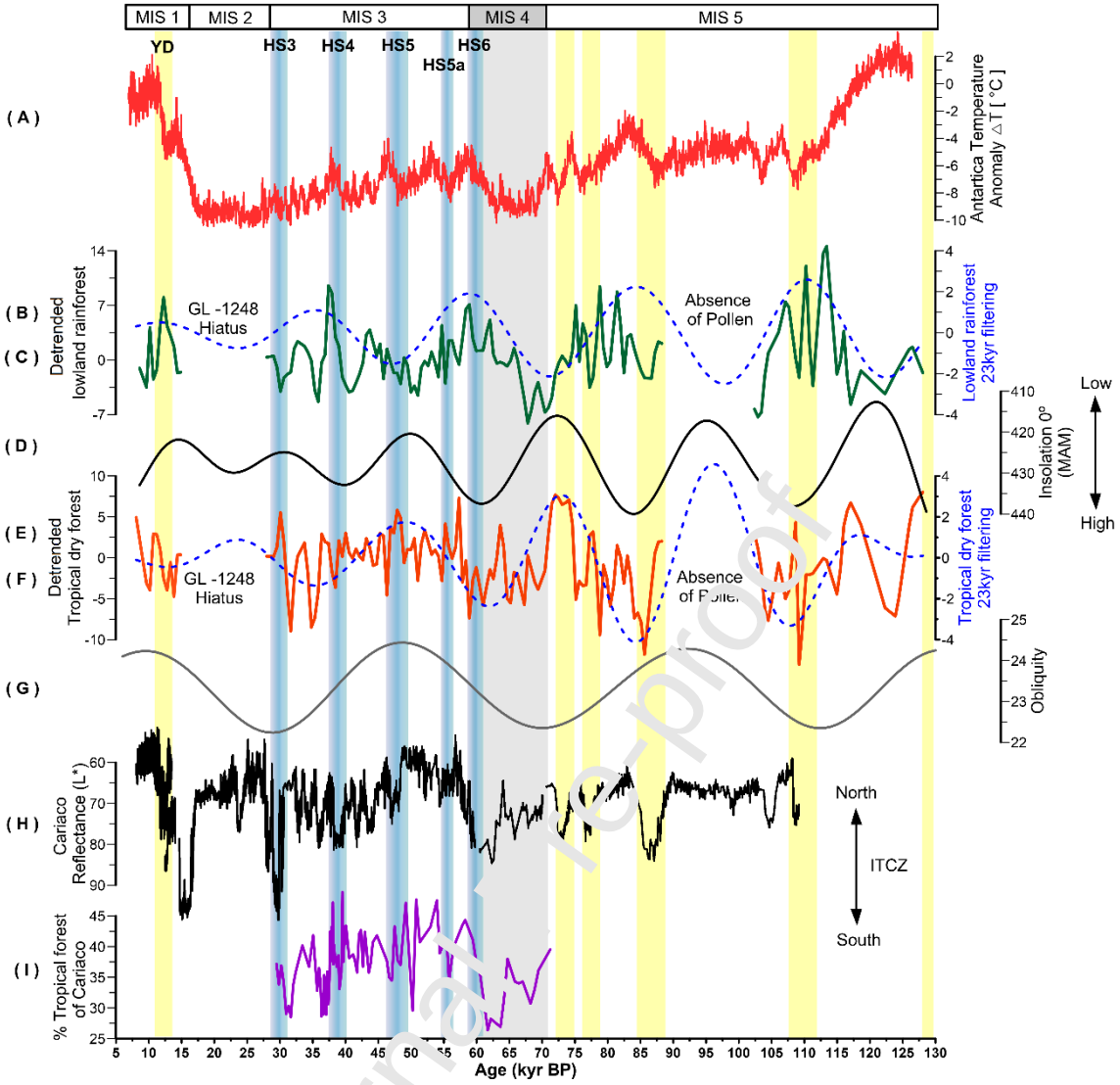

Figure 6: (A) Dome C temperature anomaly, ΔT [°C] (Petit *et al.*, 1999); (B) Detrended lowland rainforest; (C) Lowland rainforest 23 kyr bandpass filter output; (D) Inverted axis of insolation 0° (March to May), black line (Laskar *et al.*, 2004); (E) Detrended tropical dry forest; (F) Tropical dry forest 23 kyr bandpass filter output; (G) Obliquity orbit, black dotted line (Berger & Loutre, 1999); (H) Reflectance L* of Cariaco Basin (Deplazes *et al.*, 2013); (I) %Tropical forest of Cariaco Basin (Gonzalez *et al.*, 2008; Hessler *et al.*, 2010); Shadings indicate the 95% confidence interval calculated after Maher (1972). The Heinrich Stadials (HS) are marked in light blue, with the respective acronyms. The MIS 4 is marked in gray, the Younger Dryas (YD) and the other Stadials of the early glacial (~70 - 115 kyr) and the last interglacial (MIS5e, ~115 -130 kyr). The 23 kyr cycles were extracted with LOESS bandpass filter using free Acycle software (Li *et al.*, 2019).

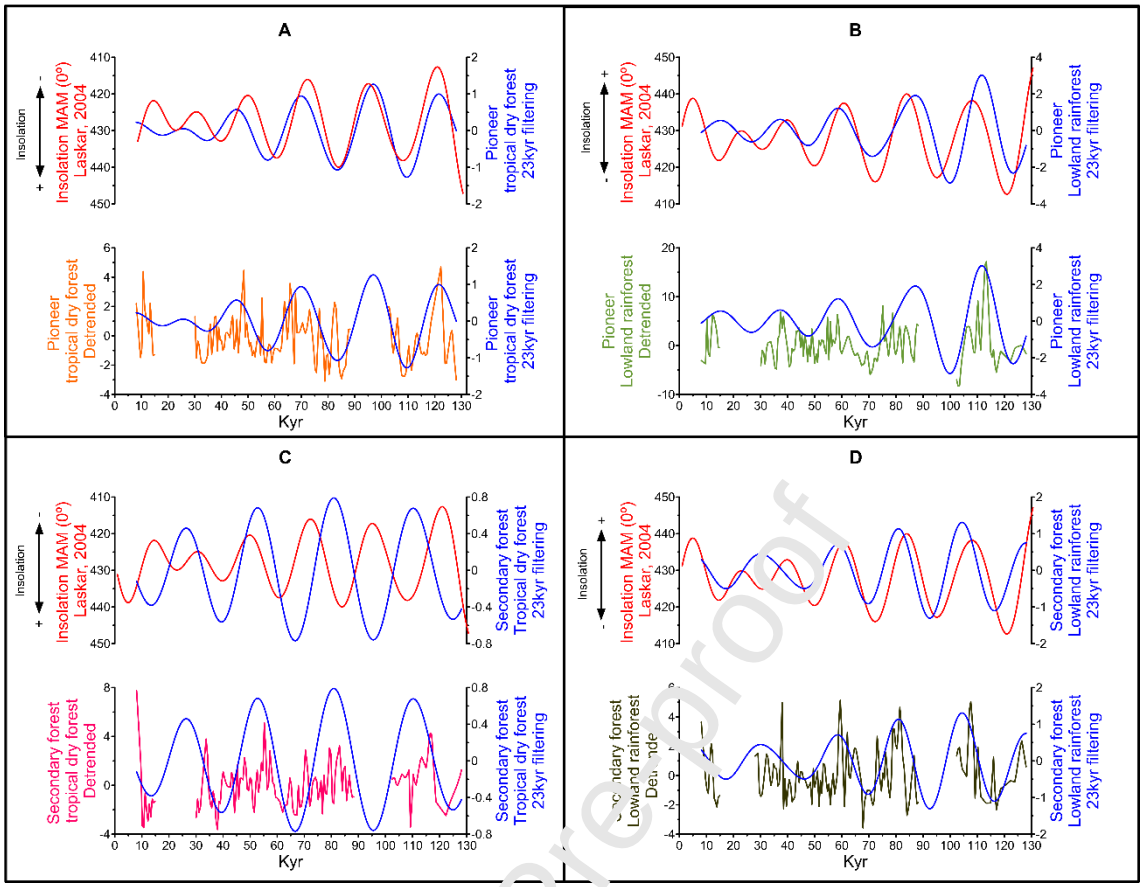

Figure 7: (A) Detrended pioneer trees of the tropical dry forest; (B) Detrended pioneer trees lowland rainforest; (C) Detrended secondary forest of the tropical dry forest; (D) Detrended secondary forest of lowland rainforest. The inverted axis of insolation 0° MAM for tropical dry forest (red line), and the insolation 0° MAM for lowland rainforest (red line). The 23 kyr cycles were extracted with LOESS bandpass filter (blue line) for each arboreal pollen group.

Wetland	Lowland rainforest		Tropical dry forest (*caatinga and cerrado*)	
▪ Cyperaceae, ▪ Iridaceae, ▪ *utricularia* (Lentibulariaceae), ▪ *Ludwigia* (Onagraceae), ▪ Polygonaceae	▪ *Alchornea* (Euphorbiaceae), ▪ *Allophylus* (Sapindaceae), ▪ Arecaceae, ▪ *Banara* (Flacourtiaceae), ▪ Bombacaceae, ▪ *Cecropia* (Urticaceae), ▪ *Celtis* (Cannabaceae), ▪ *Cordia* (Boraginaceae), ▪ Curcubitaceae, ▪ *Dioclea* (Fabaceae), ▪ *Doliocarpus type* (Dilleniaceae), ▪ Flacourtiaceae, ▪ *Gallesia* (Phytolaccaceae), ▪ *Gordonia* (Theaceae), ▪ *Hippocratea volubilis*	▪ Malpighiaceae, ▪ *Mauritia* (Arecaceae), ▪ Meliaceae, ▪ Menispermaceae, ▪ Moraceae-Urticaceae, ▪ *Mucuna* (Fabaceae), ▪ Myrtaceae, ▪ Piperaceae, ▪ Proteaceae, ▪ *Protium* (Burseraceae), ▪ *Salix* (Salicaceae), ▪ *Sebastiana brasiliensis* (Euphorbiaceae), ▪ *Solanum* (Solanaceae), ▪ *Symphonia Globulifera* (Clusiaceae), ▪ *Zanthoxylum* (Rutaceae)	▪ Acanthaceae, ▪ *Aegiphila* (Verbenaceae), ▪ *Alternanthera* (Amaranthaceae), ▪ Amaranthaceae/Chenopodiaceae, ▪ Anacardiaceae, ▪ Annonaceae, ▪ Apocynaceae, ▪ Asteraceae, ▪ *Bauhinia* (Fabaceae), ▪ Boraginaceae, ▪ Borreria (Rubiaceae), ▪ *Byrsonima* (Malpighiaceae), ▪ Cactaceae, ▪ Convolvulaceae, ▪ *Cuphea* (Lythraceae), ▪ *Didymopanax* (Araliaceae), ▪ *Faramae* (Rubiaceae), ▪ *Gomphrena-Pfaffia type* (Amaranthaceae),	▪ *Justicia pectoralis* (Acanthaceae), ▪ *Kallstroemia* (Zygophyllaceae), ▪ Lamiaceae, ▪ Lauraceae, ▪ Malvaceae, ▪ *Matricaria* (Anthemideae) ▪ Mimosaceae, ▪ *Psychotria* (Rubiaceae), ▪ Rhamnaceae, ▪ Rubiaceae, ▪ Scrophulariaceae, ▪ Spermacoceae, ▪ Sterculiaceae, ▪ *subf. Asteoideae* (Asteraceae), ▪ *subf. Cichorioideae* (Asteraceae), ▪ *Trichocline* (Asteraceae), ▪ Turneraceae, ▪ *Vitis tiliifolia*

	(Celastraceae),	(Vitaceae)

Table 1 - The list of the most representative groups (wetland, lowland rainforest, and tropical dry forest) of pollen taxa identified in marine sediment core GL-1248. The pollen taxa are grouped according to their phytogeographical assignment based on De Oliveira *et al.* (1999), Behling *et al.* (2000), and Bouimetarhan *et al.* (2018).

Name		Structure	Succecion type
Tropical dry forest			
Annonaceae		Trees and shrubs	Pionner
Araliaceae	*Didymopanax*	Trees and shrubs	Pionner
Boranginaceae		Lianas	Pionner
Cactaceae		Trees and shrubs	Pionner
Convolvulaceae		Lianas	Pionner
Mimosaceae		Trees and shrubs	Pionner
Rubiaceae	*Psychotria*	Trees and shrubs	Pionner
Verbenaceae		Lianas	Pionner
Lowland rainforest			
Arecaceae		Trees and shrubs	Pionner
Arecaceae	*Mauritia*	Trees and shrubs	Pionner
Bombacaeae		Trees and shrubs	Pionner
Boranginaceae	*Cordia*	Tree to herb	Pionner
Euphorbiaceae	*Alchornea*	Trees and shrubs	Pionner
Malpighiaceae		Shrubs	Pionner
Meliaceae		Trees and shrubs	Pionner
Myrtaceae		Trees	Pionner
Melastomataceae/ Combrataceae		Trees and shrubs	Pionner
Phytolaccaceae	*Gallesia*	Trees	Pionner
Piperaceae	*Piper*	Trees	Pionner
Proteaceae		Trees and shrubs	Pionner
Rutaceae	*Zanthoxylum*	Trees and shrubs	Pionner
Salicaceae	*Salix*	Trees and shrubs	Pionner
Sterculiaceae		Trees and shrubs	Pionner
Ulmeaceae		Trees	Pionner
Urticaceae	*Cecropia*	Shrubs	Pionner

Name	Structure	Succecion type
Tropical dry forest		
Anacardiaceae	Trees and shrubs	Secondary forest
Apocynaceae	Trees	Secondary forest

Lythraceae	*Cuphea*	Shrubs	Secondary forest
Malpighiaceae	*Byrsonima*	Shrubs	Secondary forest
Malvaceae		Trees and shrubs	Secondary forest
Rubiaceae	*Faramea*	Trees and shrubs	Secondary forest
Vitaceae	*vitis tiliifolia*	Trees	Secondary forest
Lowland rainforest			
Burseraceae	*Protium*	Trees and shrubs	Secondary forest
Cannabaceae	*Celtis*	Trees and shrubs	Secondary forest
Celastraceae	*H. volubilis*	Lianas	Secondary forest
Curcubitaceae		Lianas	Secondary forest
Dilleniaceae	*Doliocarpus*	Trees and shrubs	Secondary forest
Flacourtiaceae		Trees and shrubs	Secondary forest
Menispermaceae		Epiphyte	Secondary forest
Moraceae - Urticaceae		Trees and shrubs	Secondary forest
Piperaceae		Shrubs or epiphyte	Secondary forest
Sapindaceae	*Allophylus*	Trees and shrubs	Secondary forest
Solanaceae	*Solanum*	Shrubs	Secondary forest
Symphonia	*Globulifera*	Trees and shrubs	Secondary forest
Theaceae	*Gordonia*	Trees and shrubs	Secondary forest

Table 2 – The ecological succession of the tree and shrub species from the dry forest and lowland rainforest groups, according to Gentry, 1993 and Marchant *et al.*, 2002.

Declaration of interests

The authors declare that they have no known competing financial interests or personal relationships that could have appeared to influence the work reported in this paper.

Highlights

• We discuss vegetation change and how it reflects hydrological changes within the Parnaíba Basin, northeastern (NE) Brazil, over the past 130 kyrs

• Geochemical proxies (Fe/K ratio and ƐNd) in core GL-1248 are synchronous with reconstructed vegetation patterns, highlighting periods of enhanced or reduced local soil erosion during hydrological disturbances

• We define three major vegetation groups (tropical dry forest, lowland rainforest, and wetland), and the discrepancy in water requirements between tropical dry forests and lowland rainforests is discussed

• Analysis of the hydroclimatic mechanisms in NE Brazil that triggered the succession of vegetation during glacial phases is discussed